Electronic Supplementary Material (ESI) for Organic & Biomolecular Chemistry.

Fluorescent sensing of non-steroidal anti-inflammatory drugs naproxen and ketoprofen by dansylated squaramide-based receptors

Giacomo Picci, M. Carla Aragoni, Massimiliano Arca, Claudia Caltagirone, Mauro Formica, Vieri Fusi, Luca Giorgi, Filippo Ingargiola, Vito Lippolis, Eleonora Macedi, Luca Mancini, Liviana Mummolo, and Luca Prodi

Summary

1. Materials and methods

All reactions were performed in oven-dried glassware under a slight positive pressure of nitrogen. ^{1}H-NMR (600 MHz, 400 MHz) and ^{13}C NMR (151 MHz, 100 MHz) spectra were determined on a 600 MHz Bruker and on a 400 MHz Bruker Avance instrument. NMR spectra were recorded at 298 K, chemical shifts for ^{1}H NMR were reported in parts per million (ppm), referenced relative to residual proton in the deuterated solvent, with coupling constants reported in Hertz (Hz). ^{1}H-^{1}H and ^{1}H-^{13}C correlation experiments were performed using standard Bruker pulse sequence to assign the signals. The following abbreviations were used for spin multiplicity: s = singlet, d = doublet, t = triplet, q = quartet, quint = quintet, m = multiplet, dd = doublet of doublets, br = broad signal. Chemical shifts for ^{13}C NMR spectra were reported in ppm, relative to the central line of a septet at δ = 39.52 ppm for deuterated dimethylsulfoxide.

UV−Vis absorption spectra were recorded using a Perkin-Elmer Lambda 45 spectrophotometer. The fluorescence spectra were recorded with a Perkin Elmer LS-55 spectrofluorometer, (λ_{exc} = 350 nm). Time correlated single photon counting experiments were conducted on an Edinburgh FLS920 equipped with a photomultiplier Hamamatsu R928P and connected to a PCS900 PC card (λ_{exc} = 340 nm. λ_{em} = 525 nm). Luminescence quantum yields were determined using fluorescein solution in NaOH 0.1 M as a reference (Φ = 0.92). All measurements were performed at 298.0 ± 0.1 K, with ligand concentrations $1\cdot10^{-5}$ M. Quartz cuvettes with optical path length of 1 cm were used.

All solvents and starting materials were purchased from commercial sources where available. Compounds **2** and **11** were synthesized as reported in the literature.[1] Proton NMR titrations were performed by adding aliquots of a putative anionic guest (such as the sodium salt, $7.5\cdot10^{-2}$ M) in a solution of the receptor ($5.0\cdot10^{-3}$ M) in DMSO-d_6/0.5% water. Quantum-chemical calculations were carried out on the BzO^- and KET^- anions, on the ligands **L2** and **L4** and on the 1:1 adducts **L2**·BzO^-, **L2**·KET^-, **L4**·BzO^-, and **L4**·KET^-. Calculations were carried out at the density functional theory (DFT)[2] level with the commercial suite Gaussian 16,[3] with the hybrid mPW1PW functional,[4] including a modified Perdew and Wang (PW) exchange functional coupled with the PW correlation functional.[5] Schäfer, Horn, and Ahlrichs split-valence plus polarization[6] all-electron basis sets were used in the Weigend formulation Def2SVP.[7] The geometry of all compounds was optimized. The nature of the minima of each structure was verified by harmonic frequency calculations. TD-DFT calculations were carried out at the optimized geometries. GaussView 6.0.16[8] was used to draw Kohn-Sham (KS) molecular orbital (MO) compositions, to generate molecular electrostatic potential maps, to analyse natural charge distributions, and to prepare TD-simulated spectra and calculate molar extinction coefficients from oscillator strengths . Association constants were obtained by using the open source program Bindift (http://app.supramolecular.org/bindfit/).

References

1 M. A. Ilies, W. A. Seitz, B. H. Johnson, E. L. Ezell, A. L. Miller, E. B. Thompson and A. T. Balaban, Journal of Medicinal Chemistry, 2006, 49, 3872-3887

2 W. Koch,M. C. Holthausen, “A Chemist’s Guide to Density Functional Theory”, 2nd ed.; Wiley-VCH: Weinheim, 2002.

3 Gaussian 16, Revision C.01, M. J. Frisch, G. W. Trucks, H. B. Schlegel, G. E. Scuseria, M. A. Robb, J. R. Cheeseman, G. Scalmani, V. Barone, G. A. Petersson, H. Nakatsuji, X. Li, M. Caricato, A. V. Marenich, J. Bloino, B. G. Janesko, R. Gomperts, B. Mennucci, H. P. Hratchian, J. V. Ortiz, A. F. Izmaylov, J. L. Sonnenberg, D. Williams-Young, F. Ding, F. Lipparini, F. Egidi, J. Goings, B. Peng, A. Petrone, T. Henderson, D. Ranasinghe, V. G. Zakrzewski, J. Gao, N. Rega, G. Zheng, W. Liang, M. Hada, M. Ehara, K. Toyota, R. Fukuda, J. Hasegawa, M. Ishida, T. Nakajima, Y. Honda, O. Kitao, H. Nakai, T. Vreven, K. Throssell, J. A. Montgomery, Jr., J. E. Peralta, F. Ogliaro, M. J. Bearpark, J. J. Heyd, E. N. Brothers, K. N. Kudin, V. N. Staroverov, T. A. Keith, R. Kobayashi, J. Normand, K. Raghavachari, A. P. Rendell, J. C. Burant, S. S. Iyengar, J. Tomasi, M. Cossi, J. M. Millam, M. Klene, C. Adamo, R. Cammi, J. W. Ochterski, R. L. Martin, K. Morokuma, O. Farkas, J. B. Foresman, and D. J. Fox, Gaussian, Inc., Wallingford CT, 2016.

4 C. Adamo, V. Barone, “Exchange functionals with improved long-range behavior and adiabatic connection methods without adjustable parameters: The mPW and mPW1PW models”, J. Chem. Phys. 108, 664 (1998)

5 J. P. Perdew, K. Burke, Y. Wang, “Generalized gradient approximation for the exchange-correlation hole of a many-electron system” Phys. Rev. B, 54, 16533–16539 (1996).

6 A. Schäfer, H. Horn, R. Ahlrichs, “Fully optimized contracted Gaussian basis sets for atoms Li to Kr”, J. Chem. Phys. 97, 2571 (1992)

7 F. Weigend, R. Ahlrichs, “Balanced basis sets of split valence, triple zeta valence and quadruple zeta valence quality for H to Rn: Design and assessment of accuracy”, Phys. Chem. Chem. Phys., 2005,7, 3297-3305

8 R. Dennington, T.A. Keith, J.M. Millam, GaussView, Version 6, Semichem Inc., Shawnee Mission, KS, 2016.

2. Synthetic procedures

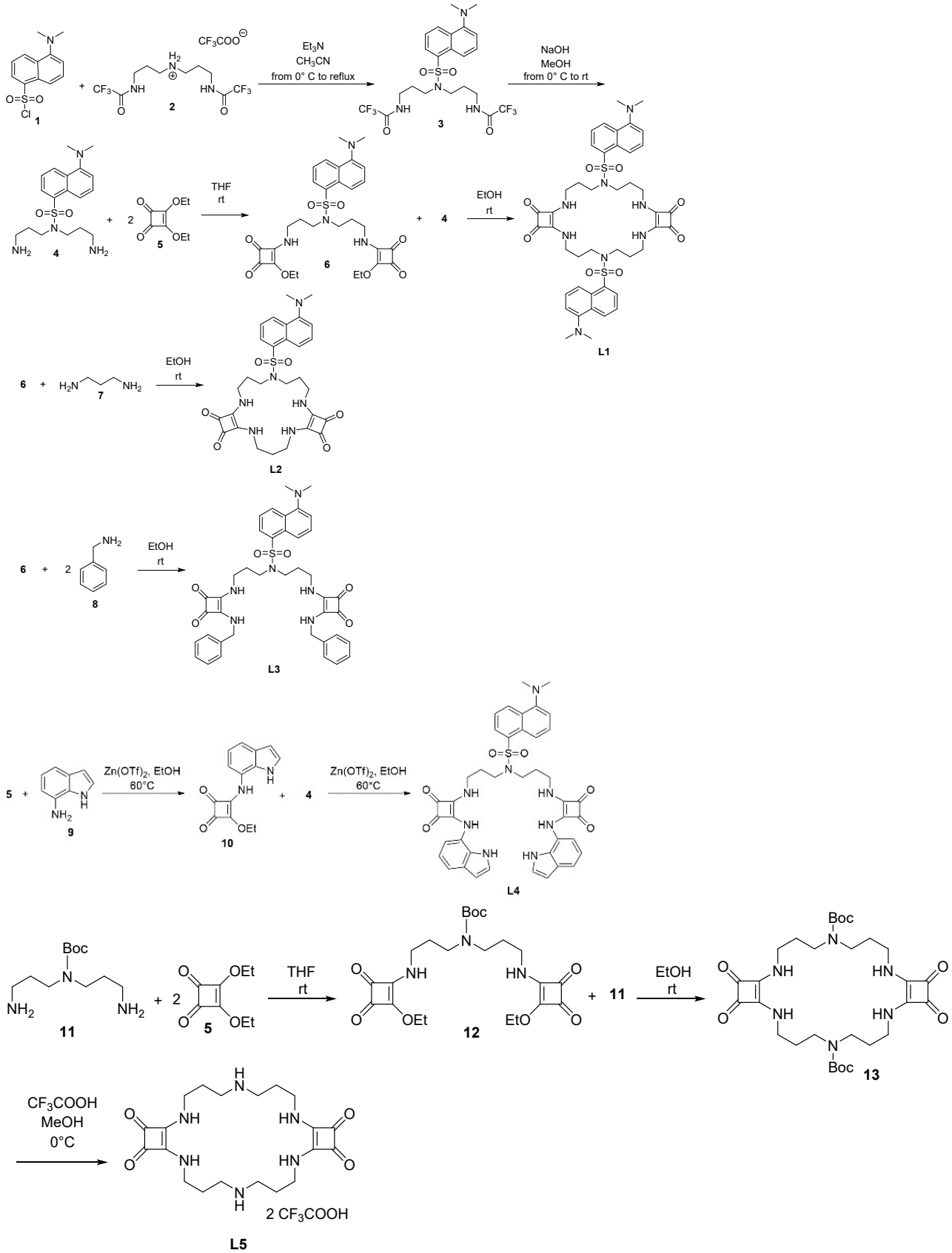

Scheme S1. Synthetic pathways to obtain **L1-L5**.

Synthesis of N,N-bis(3-trifluoroacetylamino)propyl)-5-(dimethylamino)naphthalene-1-sulfonamide (3)

A solution of 5-(dimethylamino)naphthalene-1-sulfonyl chloride (**1**) (dansyl chloride, 3.56 g, 12 mmol) in acetonitrile (200 mL) was added dropwise, in a nitrogen atmosphere, to a stirred solution of N,N-bis(3-trifluoroacetylamino)propyl)amine (**2**) (5 g, 11 mmol) in triethylamine (5 mL, 35 mmol) and refluxed overnight. The resulting mixture was filtered to remove the insoluble salts, concentrated under reduced pressure to 50 mL and poured in 200 mL of cold water. The resulting suspension was extracted with ethyl acetate (3x50 mL), the combined organic extracts were dried with anhydrous Na_2SO_4 and evaporated under reduced pressure affording 6 g of a grey/greenish solid which was purified by crystallization from hot ethanol to obtain **3** as white/green needle-like crystals (3.46 g. 54%).

^{1}H-NMR (400 MHz, $CDCl_3$) δ (ppm) = 1.84 (quint, 4H, *J* = 6.4 Hz), 2.90 (s, 6H), 3.38 (t, 4H, *J* = 6.4 Hz), 3.45 (q, 4H, *J* = 6.5 Hz), 7.03 (br s, 2H), 7.22 (d, 1H, *J* = 7.6 Hz), 7.55 (dd, 1H, J_1=8.5 J_2=7.5 Hz), 7.60 (dd, 1H, J_1 = 8.6 J_2 = 7.6 Hz), 8.04 (dd, 1H, J_1 = 7.3 J_2 = 1.3 Hz), 8.23 (d, 1H, *J* = 8.8 Hz), 8.59 (d, 1H, *J* = 8.6 Hz).

Synthesis of N,N-bis(3-aminopropyl)-5-(dimethylamino)naphthalene-1-sulfonamide (4)

120 mL of 0.2 M sodium hydroxide in methanol was dropwise added to a stirred solution of **3** (3.46 g, 6.22 mmol) in 500 mL of methanol at 0 °C under nitrogen atmosphere. When the addition was complete, the cooling bath was removed, and the mixture was stirred at overnight at room temperature. The solvent was evaporated under reduced pressure obtaining an oily residue that was suspended in 100 mL of water and extracted with chloroform (4 x 150 mL). The combined organic extracts were dried with anhydrous Na_2SO_4 and evaporated under reduced pressure to obtain **4** as a yellow/orange oil (2.46 g, 100%).

^{1}H-NMR (400 MHz, $CDCl_3$) δ (ppm) = 1.58 (br s, 4H), 1.64 (quint, 4H, *J* = 7.0 Hz), 2.62 (t, 4H, *J* = 6.7), 2.87 (s, 6H), 3.37 (t, 4H, *J* = 7.3 Hz), 7.17 (d, 1H, *J* = 7.6), 7.51 (dd, 1H, J_1 = 8.6 J_2 = 7.6 Hz), 7.55 (dd, 1H, J_1 = 8.6 J_2 = 7.6 Hz), 8.15 (dd, 1H, J_1 = 7.3 J_2 = 1.3 Hz), 8.27 (d, 1H, *J* = 8.8 Hz), 8.52 (d, 1H, *J* = 8.3 Hz).

Synthesis of N,N-bis(3-(2-ethoxy-3,4-dioxocyclobut-1-en-1-yl)aminopropyl)-5-(dimethylamino)naphthalene-1-sulfonamide (6)

Over a period of 3 h a solution of 1,2-diethoxy-3,4-dioxocyclobut-1-ene (**5**) (1.26 g, 7.42 mmol) in tetrahydrofuran (60 mL) was added to a stirred solution of **4** (1.23 g, 3.37 mmol) in tetrahydrofuran (200 mL) under nitrogen atmosphere. The mixture was stirred at room temperature for 72 h, then the solvent was evaporated under reduced pressure affording a yellow/orange oil. The crude product was purified by chromatography (silica, ethyl acetate/hexane 8:2) to obtain the **6** as a yellow/orange oil (1.2 g, 58%).

^{1}H-NMR (400 MHz, $CDCl_3$) δ (ppm) = 1.42 (t, 6H, *J* = 6.9 Hz), 1.83-2.01 (m, 4H), 2.88 (s, 6H), 3.31-3.74 (m, 8H), 4.73 (q, 4H, *J* = 7.0 Hz), 7.19 (d, 1H, *J* = 7.6 Hz), 7.43 (br s, 2H), 7.48-7.62 (m, 2H), 8.06 (d, 1H, *J* = 7.1), 8.24 (t, 1H, *J* = 9.1 Hz), 8.54 (d, 1H, *J* = 7.8 Hz).

Synthesis of 6,19-bis(5-(dimethylamino)naphthalen-1-yl-sulphonyl)-12,13,25,26-tetraoxo-2,6,10,15,19,23-hexaazatricyclo[22.2.0.0(11,14)]hexaicosa-1(24),11(14)-diene (L1)

Over a period of 6 h a solution of **4** (0.18 g, 0.490 mmol) in ethanol (100 mL) was added dropwise to a stirred solution of **6** (0.30 g, 0.490 mmol) in ethanol (100 mL). The reaction mixture was stirred at room temperature for 72 h. The yellow precipitate that formed was filtered, washed with ethanol and re-crystallized from hot DMF affording pure **L1** as pale-yellow solid (0.227 g, 64%).

^{1}H NMR (400 MHz, DMSO-d_6/0.5% water) δ (ppm) = 1.65 (br s, 8H), 2.83 (s, 12H), 3.26 (t, 8H, *J* = 8.3 Hz), 3.36 (br s, 8H), 7.24 (d, 2H, *J* = 7.6 Hz), 7.56-7.66 (m, 4H), 8.09 (d, 2H, *J* = 7.1 Hz), 8.17 (d, 2H, *J* = 8.8 Hz), 8.48 (d, 2H, *J* = 8.6 Hz).). ^{13}C NMR (100 MHz, DMSO-d_6/0.5% water δ (ppm) = 182.9, 168.1, 151.9, 135.2, 130.4, 129.8, 129.7, 129.3, 128.6, 124.1, 119.2, 115.7, 45.5, 44.5, 41.3, 30.2. Elemental analysis for $C_{44}H_{52}N_8O_8S_2$: calcd C 59.71, H 5.92, N 12.66 S 7.24; found C 59.6, H 6.0, N 12.5, S 7.4. (ESI): *m/z* calcd. for $C_{44}H_{52}N_8O_8S_2$: 884.33; found: 885.2 $[M+H]^+$.

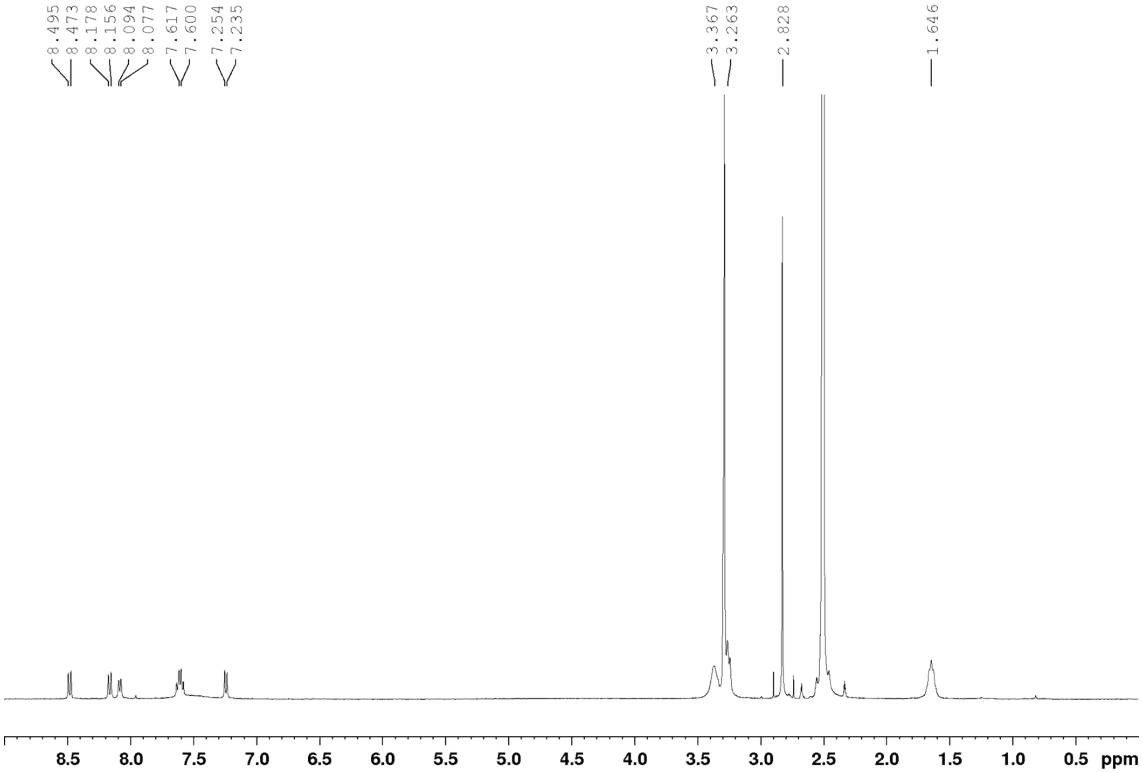

Figure S1. ^{1}H NMR spectrum of **L1** in DMSO-d_6/0.5% water solution at 298 K.

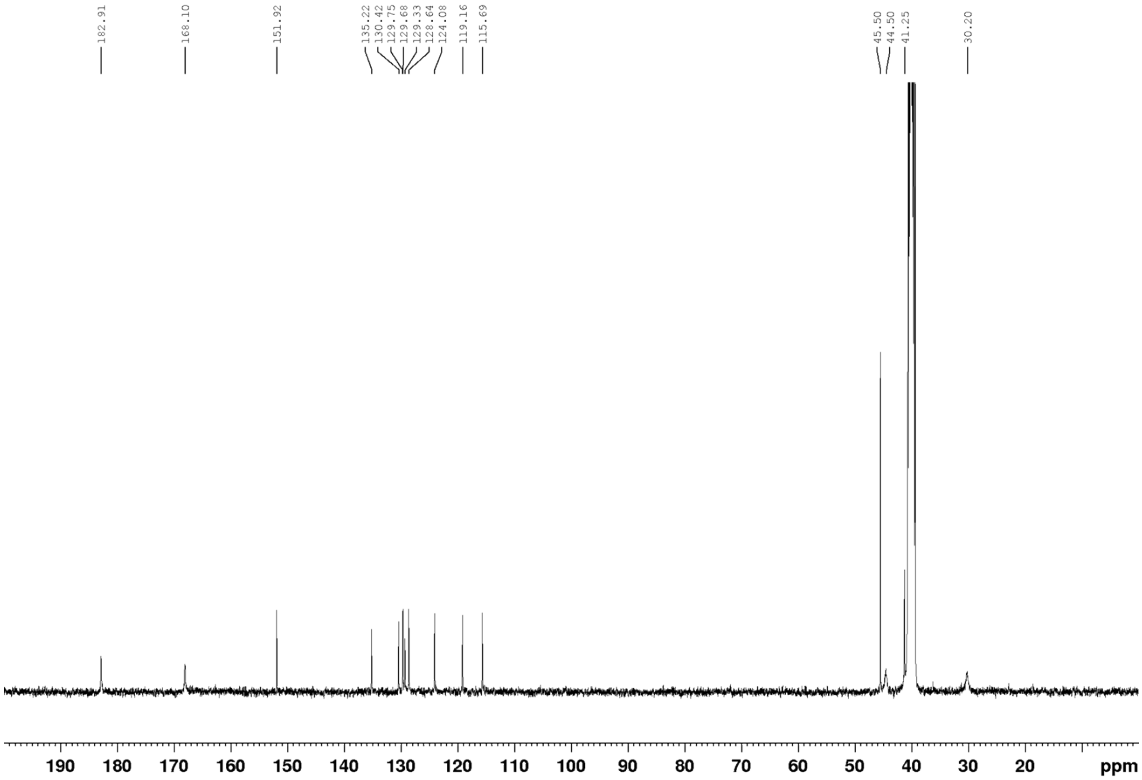

Figure S2. ^{13}C NMR spectrum of **L1** in DMSO-d_6/0.5% water solution at 298 K.

Synthesis of 6-(5-(dimethylamino)naphthalen-1-yl-sulphonyl)-12,13,21,21-tetraoxo-2,6,10,15,19-pentaazatricyclo[18.2.0.0(11,14)]doicosa-1(20),11(14)-diene (L2)

A solution of 1,3-propylendiamine (**7**) (4 mg, 0.490 mmol) in ethanol (100 mL) was added dropwise to a stirred solution of **6** (0.30 g, 0.490 mmol) in ethanol (100 mL). The reaction mixture was stirred at room temperature for 72 h. The yellow precipitate that formed was filtered, washed with ethanol and re-crystallized from hot DMF affording pure **L2** as pale-yellow solid (0.228 g, 78%).

^{1}H-NMR (400 MHz, DMSO-d_6/0.5% water): δ (ppm)= 1.64 (br s, 4H), 1.85 (br s, 2H), 2.85 (s, 6H), 3.28 (t, 4H, J = 7.3 Hz), 3.35-3.46 (m, 4H), 3.47-3.73 (br s, 4H), 7.28 (d, 1H, J = 7.3 Hz), 7.63 (dd, 1H, J_1 = 8.5 Hz J_2 = 7.7 Hz), 7.66 (dd, 1H, J_1 = 8.5 Hz J_2 = 7.5 Hz), 8.14 (d, 1H, J = 7.1 Hz), 8.21 (d, 1H, J = 8.8 Hz), 8.52 ppm (d, 1H, J = 8.3 Hz). ^{13}C NMR (100 MHz, DMSO-d_6/0.5% water) δ (ppm) = 183.2, 168.3, 152.0, 130.6, 129.8, 129.7, 128.7, 124.2, 119.2, 115.7, 45.5, 44.3, 40.8, 31.2, 30.5 ppm. Elemental analysis for $C_{29}H_{34}N_6O_6S$: calcd C 58.57, H 5.76, N 14.13 S 5.39; found C 58.5, H 5.8, N 14.0, S 5.3. (ESI): *m/z* calcd. for $C_{29}H_{34}N_6O_6S$: 594.23; found: 595.2 $[M+H]^+$.

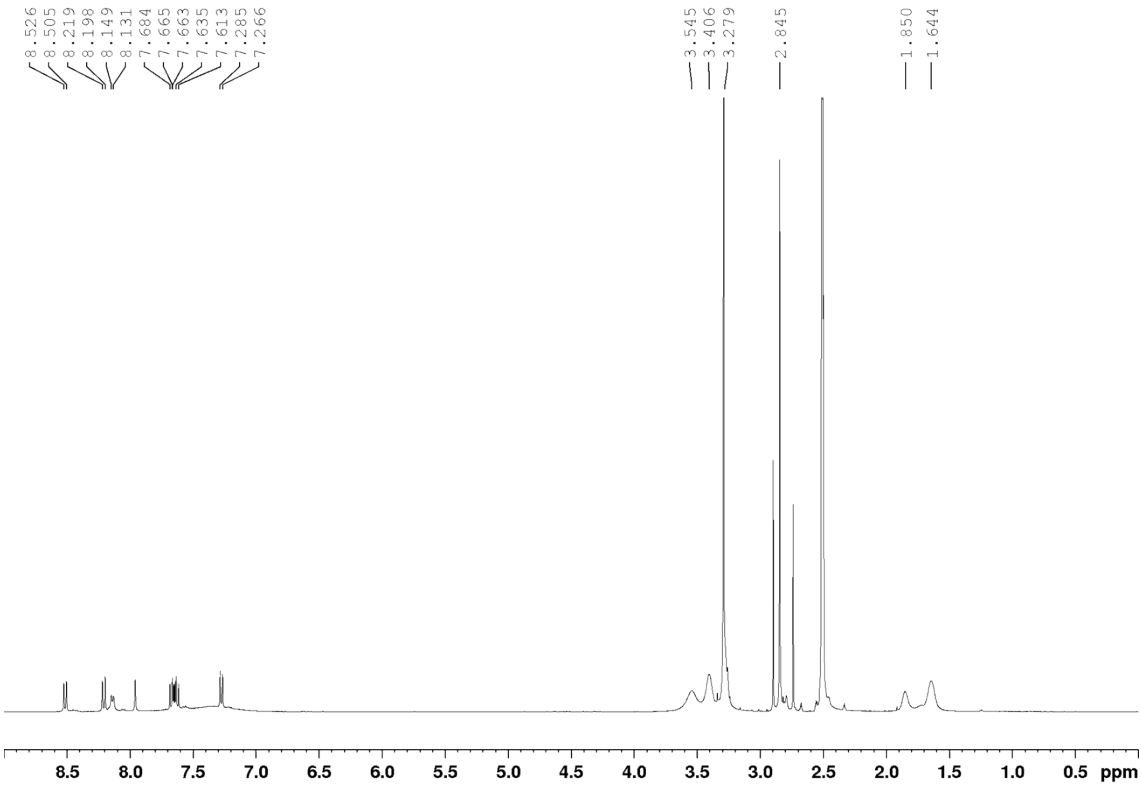

Figure S3. ^{1}H NMR spectrum of **L2** in DMSO-d_6/0.5% water solution at 298 K.

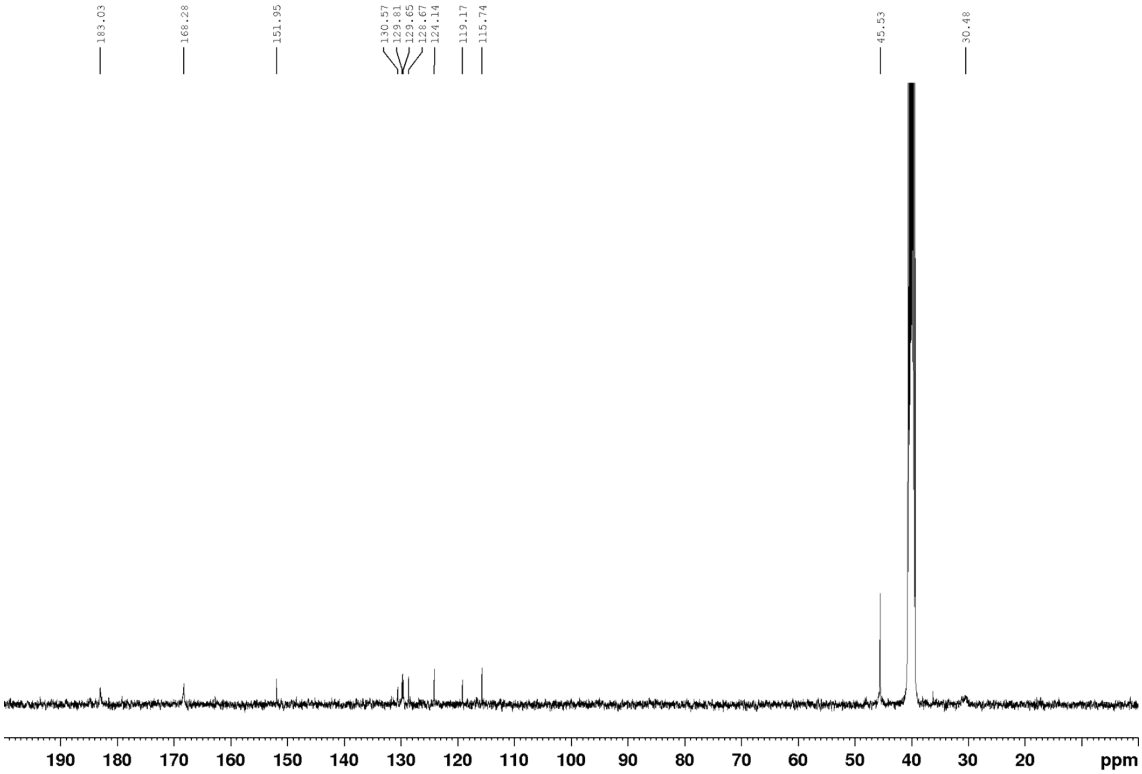

Figure S4. ^{13}C NMR spectrum of **L2** in DMSO-d_6/0.5% water solution at 298 K.

Synthesis of N,N-bis(3-(benzylamino)-3,4-dioxocyclobut-1-en-1-yl)amino)propyl)-5-(dimethylamino)naphthalene-1-sulfonamide (L3)

A solution of benzylamine (**8**) (91.0 mg, 0.84 mmol) in ethanol (50 mL) was added dropwise to a stirred solution of **6** (0.260 g, 0.42 mmol) in ethanol (50 mL). The reaction mixture was stirred for 96 h. The precipitate that formed was filtered, washed with ethanol, and re-crystallized from hot DMF affording pure **L3** as pearly-white solid (0.291 g, 93%).

^{1}H-NMR (400 MHz, DMSO-d_6/0.5% water) δ (ppm) = 1.72 (quint, 4H, *J* = 7.3 Hz, H9), 2.83 (s, 6H, H1), 3.32 (br s, 4H, H10), 3.44 (br s, 4H, H8), 4.72 (s, 4H, H13), 7.19-7.25 (m, 1H, H2), 7.25-7.41 (m, 10H, H14+H15+H16), 7.49 (t, 1H, *J* = 8.0 Hz, H5), 7.55 (t, 1H, *J* = 8.1 Hz, H3), 7.75 (br s, 2H, H12), 8.00-8.06 (m, 1H, H6), 8.15 (d, 1H, *J* = 8.6 Hz, H4), 8.40-8.46 (m, 1H, H7). ^{13}C NMR (100 MHz, DMSO-d_6/0.5% water) δ (ppm) = 183.0, 168.2, 167.9, 151.9, 139.5, 135.3, 130.3, 129.8, 129.7, 129.1, 128.6, 128.0, 127.9, 123.9, 119.1, 115.7, 47.2, 45.5, 44.9, 41.3, 30.3. Elemental analysis for $C_{40}H_{42}N_6O_6S$: calcd C 65.38, H 5.76, N 11.44 S 4.36; found C 65.3, H 5.8, N 11.3, S 4.3. (ESI): *m/z* calcd. for C40H42N6O6S: 734.29; found: 735.2 $[M+H]^+$.

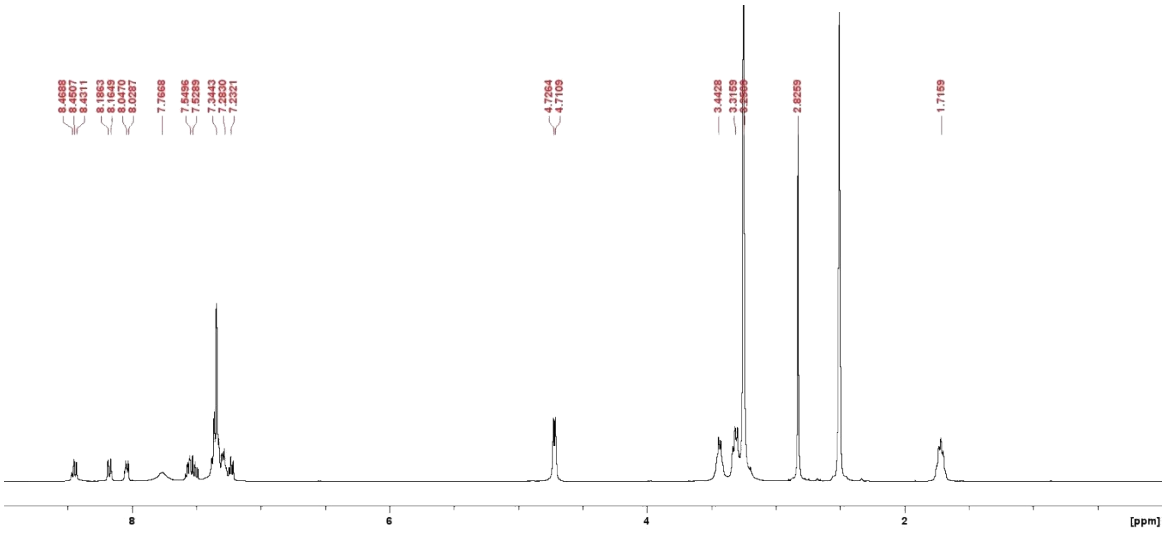

Figure S5. ^{1}H NMR spectrum of **L3** in DMSO-d_6/0.5% water solution at 298 K.

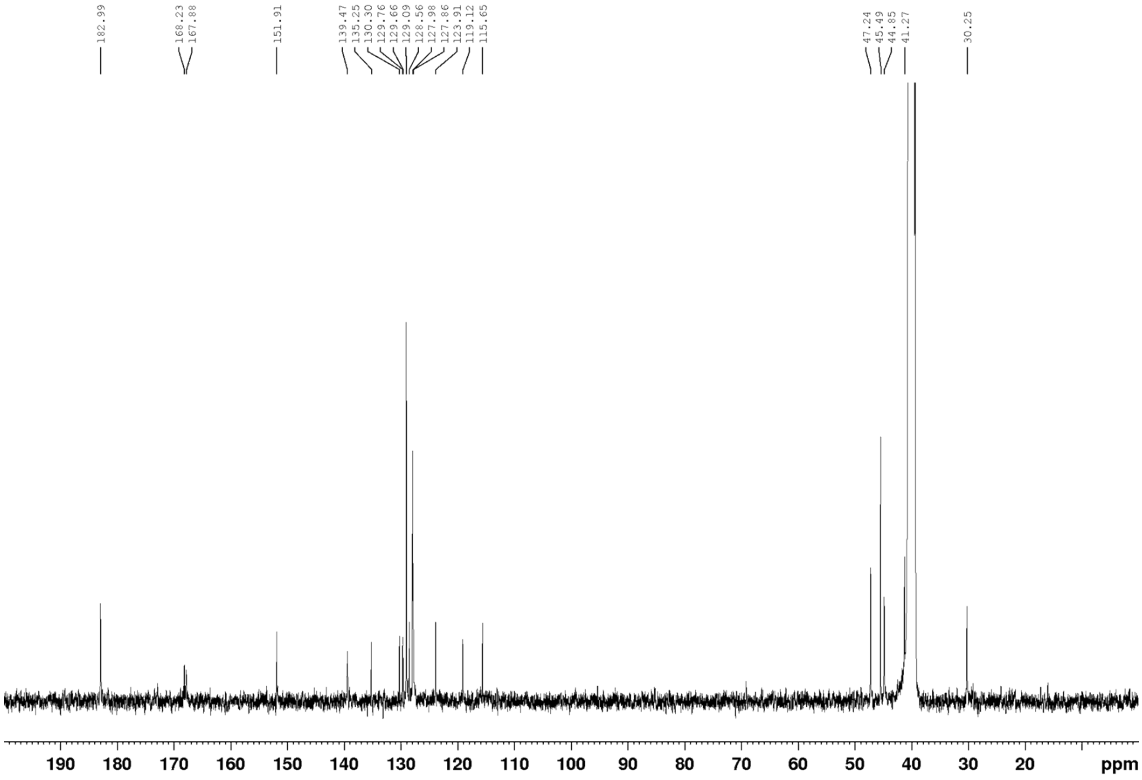

Figure S6. ^{13}C NMR spectrum of **L3** in DMSO-d_6/0.5% water solution at 298 K.

Synthesis of 3-((1H-indol-7-yl)amino)-4-ethoxycyclobut-3-ene-1,2-dione (10)

The procedure found in the literature was modified to prepare this compound. To a stirred solution of 3,4-diethoxycyclobut-3-ene-1,2-dione (200 mg, 1.18 mmol) and zinc trifluoromethanesulfonate (10 mol %) in dry ethanol (10 mL) at room temperature the 7-aminoindole (140 mg, 1.06 mmol) was added. Reaction progress was monitored by TLC chromatography (SiO_2, 1:1 hexane:ethyl acetate). Once completed, the solvent was removed under reduced pressure and the crude was purified by column chromatography (SiO_2, 3:2 hexane: ethyl acetate). The fractions containing the desired product were combined and the solvent evaporated, collecting it as crude brown solid (227 mg, 0.9 mmol). Yield: 0.25 g, 84%. ^1H NMR (600 MHz, DMSO-d_6, 298K) δ (ppm): 11.07 (s, 1H, NH), 10.57 (s, 1H, NH), 7.47 (d, *J* = 7.7 Hz, 1H, ArH), 7.44 (t, *J* = 2.3 Hz, 1H, ArH), 7.12 (s, 1H, ArH), 7.05 (t, *J* = 7.7 Hz, 1H, ArH), 6.55 (t, *J* = 2.1 Hz, 1H, ArH), 4.74 (q, *J* = 7.1 Hz, 2H, CH), 1.39 (t, *J* = 7.3 Hz, 3H, CH), ^{13}C NMR (151 MHz, DMSO-d_6, 298K) δ (ppm): 184.6, 178.7, 171.0, 129.8, 129.4, 126.23, 122.7, 119.4, 118.2, 114.9, 102.3, 69.7, 16.0. Elemental analysis % calc. for $C_{14}H_{12}N_2O_3$ (% found): C: 65.62 (65.21), H: 4.72 (4.79), N: 10.93 (10.87), O: 18.73 (19.13).

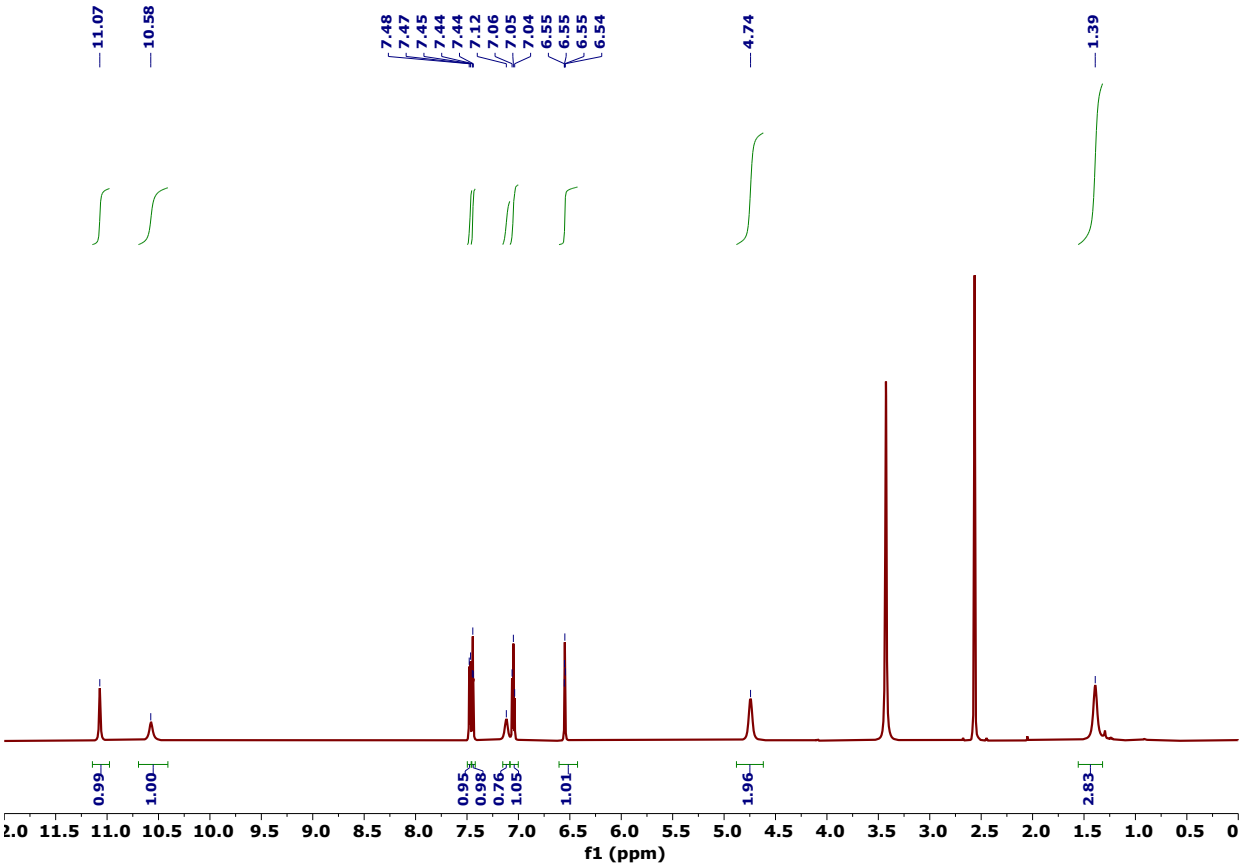

Figure S7. ^{1}H-NMR spectrum of **10** in DMSO-d_6.

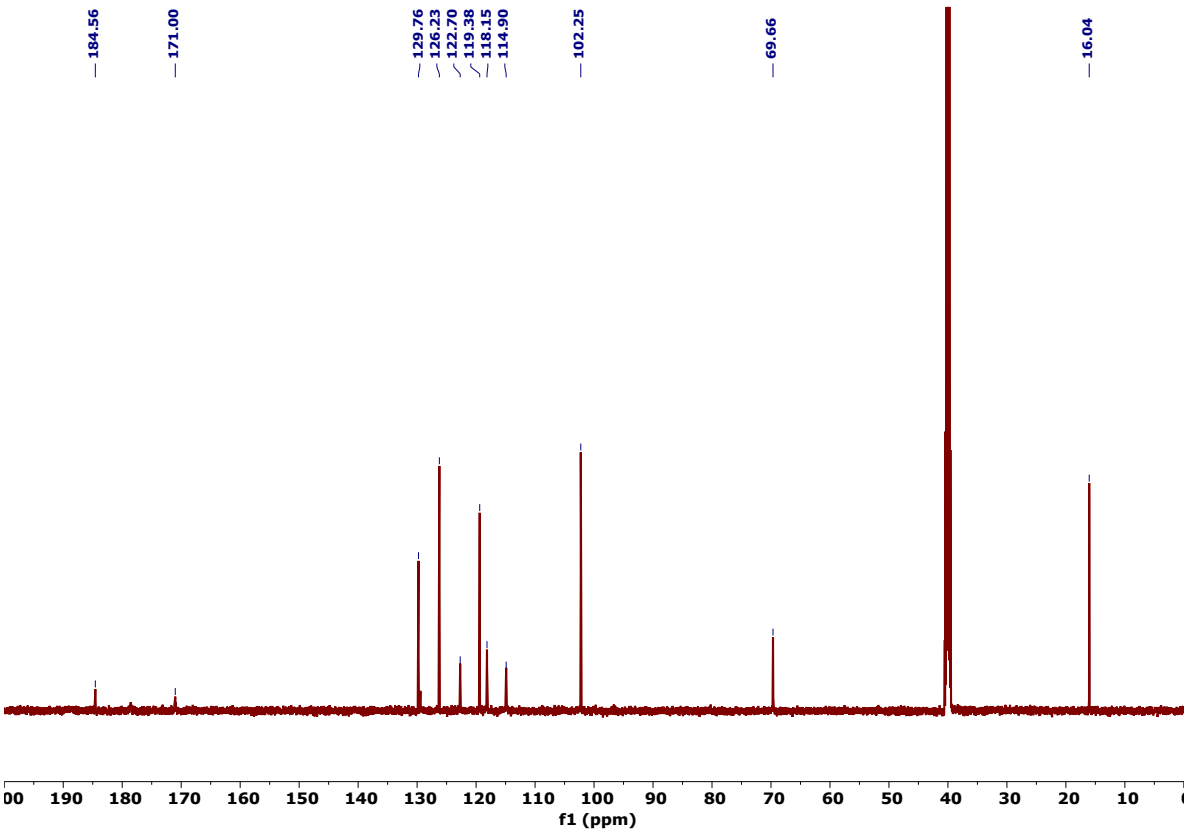

Figure S8. ^{13}C-NMR spectrum of **10** in DMSO-d_6.

Synthesis of N,N-bis(3-((2-((1H-indol-6-yl)amino)-3,4-dioxocyclobut-1-en-1-yl)amino)propyl)-5-(dimethylamino)naphthalene-1-sulfonamide (L4)

To a solution of 3-((1H-indol-7-yl)amino)-4-ethoxycyclobut-3-ene-1,2-dione (0.1828 g, 0.7133 mmol) in 30 mL of ethanol, in the presence of $Zn(OTf)_2$ (20 mol%), heated up to 60 °C. N,N-bis(3-aminopropyl)-5-(dimethylamino)naphthalene-1-sulfonamide (0.1280 g, 0.3512 mmol). A pale yellow precipitate formed immediately after the addition. The suspension was stirred for 24h. The precipitate was isolated through filtration and the product (0.175 g, 63.3%) was used without further purification. M.p. (209 °C with decomposition). ^{1}H-NMR (600 MHz, DMSO-d_6/0.5% water) δ = 10.93 (s, 2H), 9.50 (s, 2H), 8.44 (d, *J* = 12 Hz, 2H), 8.17 (d, *J* = 12 Hz, 2H), 8.05 (d, *J* = 12 Hz, 1H), 7.58 (m, 2H), 7.38 (s, 2H), 7.33 (d, *J* = 12 Hz, 2H), 7.25 (s, 2H), 7.23 (s, 2H), 6.94 (m, 4H), 6.47 (s, 2H), 3.55 (s, 4H), 3.36 (s, 4H), 2.81 (s, 6H), 2.08 (s, 12H). ^{13}C NMR (151 MHz, DMSO-d_6/0.5% water) δ = 206.9, 182.0, 151.9, 135.4, 130.3, 129.8, 129.7, 128.9, 128.6, 126.2, 124.0, 123.5, 119.8, 119.2, 117.0, 115.7, 102.4, 45.5, 45.2, 41.7, 31.2. Elemental analysis % calc. for $C_{42}H_{40}N_8O_6S$ (% found): C: 64.27 (64.21), H: 5.14 (5.19), N: 14.28 (14.30), O: 12.23 (12.26), S: 4.08 (4.11). (ESI$^-$): *m*/*z*: exp: 783.3 [M-H]$^-$ calc: 879 [M-H + DMSO+H_2O]$^-$

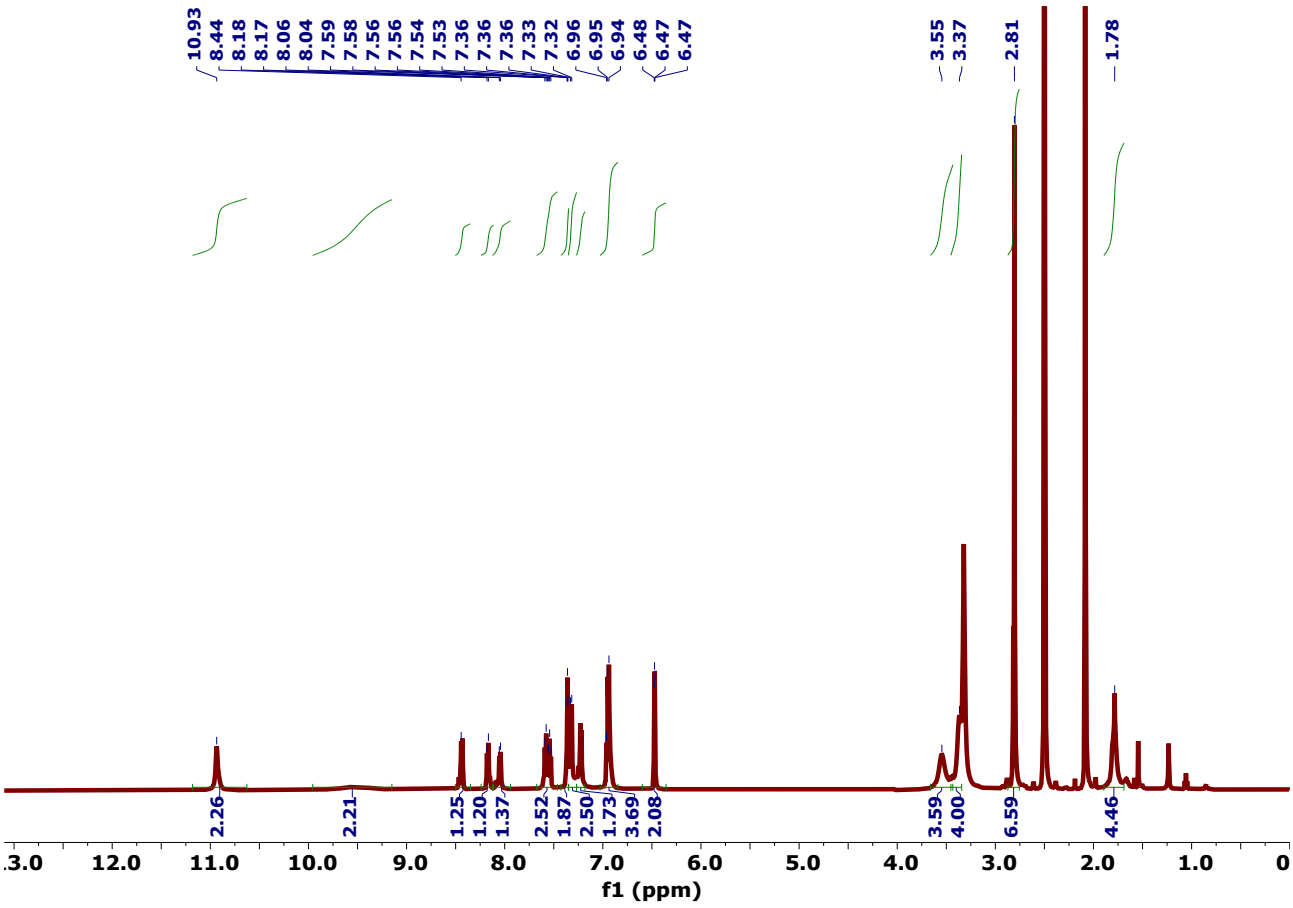

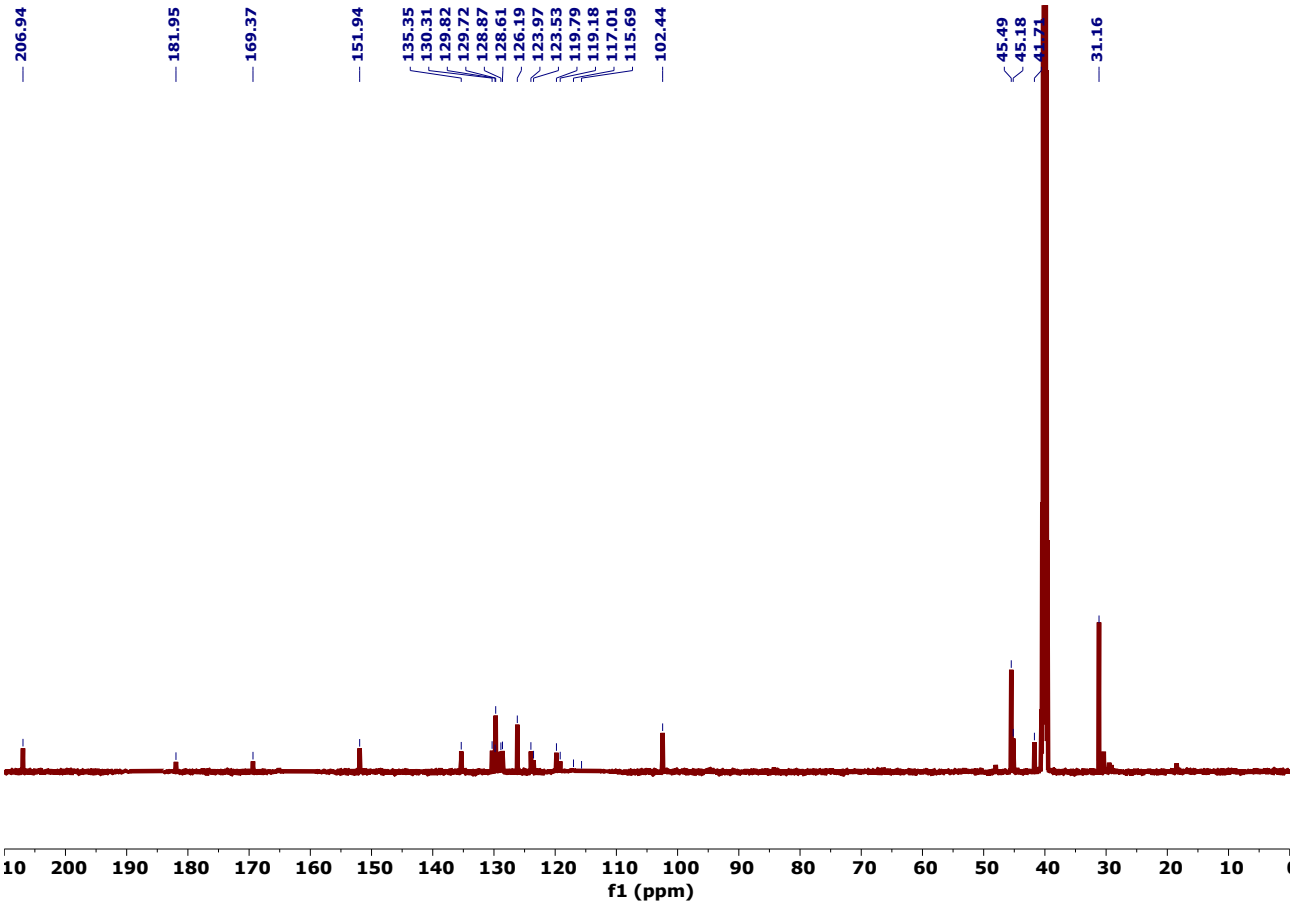

Figure S9. ^{1}H-NMR and ^{13}C-NMR spectra of **L4** in DMSO-d_6.

Synthesis of tert-butyl N,N-bis(3-(2-ethoxy-3,4-dioxocyclobut-1-en-1-yl)aminopropyl)carbamate (12)

Over a period of 3 h a solution of 1,2-diethoxy-3,4-dioxocyclobut-1-ene (**5**) (4.45 g, 26.2 mmol) in tetrahydrofuran (50 mL) was added to a stirred solution of **11** (2.75 g, 11.9 mmol) in tetrahydrofuran (60 mL) under nitrogen atmosphere. The mixture was stirred at room temperature for 96 h, then the solvent was evaporated under reduced pressure affording a yellow oil. The crude product was triturated with ethyl ether and filtered to obtain **12** as a pale yellow wax (5.1 g, 89%).

^{1}H-NMR (400 MHz, $CDCl_3$) δ (ppm)= 1.41-1.50 (m, 13H), 1.85 (t, 6H, *J* = 6.9 Hz), 3.33 (br s, 4H), 3.47 (br s, 2H), 3.63 (br s, 2H), 4.74 (q, 4H, *J* = 7.0 Hz), 7.55 (br s, 1H).

Synthesis of 6,19-bis(*tert*-butyloxycarbonyl)-12,13,25,26-tetraoxo-2,6,10,15,19,23-hexaazatricyclo[22.2.0.0(11,14)]hexaicosa-1(24),11(14)-diene (13)

Over a period of 6 h a solution of **11** (0.19 g, 0.83 mmol) in ethanol (100 mL) was added dropwise to a stirred solution of **12** (0.40 g, 0.83 mmol) in ethanol (100 mL). The reaction mixture was stirred at room temperature for 72 h. The pale yellow precipitate that formed was filtered, washed with ethanol affording pure **13** as pale-yellow solid (0.34 g, 66%).

^{1}H-NMR (400 MHz, DMSO) δ (ppm) = 1.37 (s, 9H), 1.72 (br s, 8H), 3.18 (br s, 8H), 3.47 (br s, 8H), 7.43 ppm (br s, 4H). ^{13}C NMR (100 MHz, DMSO) δ (ppm) = 186.6, 158.4, 149.2, 78.8, 49.4, 43.3, 31.5, 28.9.

Synthesis of 12,13,25,26-tetraoxo-2,6,10,15,19,23-hexaazatricyclo[22.2.0.0(11,14)]hexaicosa-1(24),11(14)-diene bis trifluoroacetate (L5·2CF_3COOH)

Compound **13** (0.34g, 0.55 mmol) was dissolved in 5 mL of trifluoroacetic acid cooled at 0°C and vigorously stirred for 8 h to warm at room temperature. The reaction mixture was added dropwise to 100 mL of diethyl ether in an ice bath obtaining the trifluoroacetate salt of **L5** as white solid that was filtered and washed with cold diethyl ether. Obtained 0.35 g of **L5·2CF_3COOH** (quantitative yield)

^{1}H-NMR (400 MHz, DMSO-d_6/0.5% water) δ (ppm) = 1.82 (br s, 8H), 2.91 (br s, 8H), 3.61 (br s, 8H), 7.68 (br s, 4H), 8.45 (br s, 4H), ^{13}C NMR (100 MHz, DMSO-d_6/0.5% water) δ (ppm) = 182.9, 168.4, 45.1, 40.6, 28.1. Elemental analysis for $C_{24}H_{32}N_6O_8F_6$: calcd C 44.59, H 4.99, N 13.00; found C 44.5, H 5.1, N 12.9.

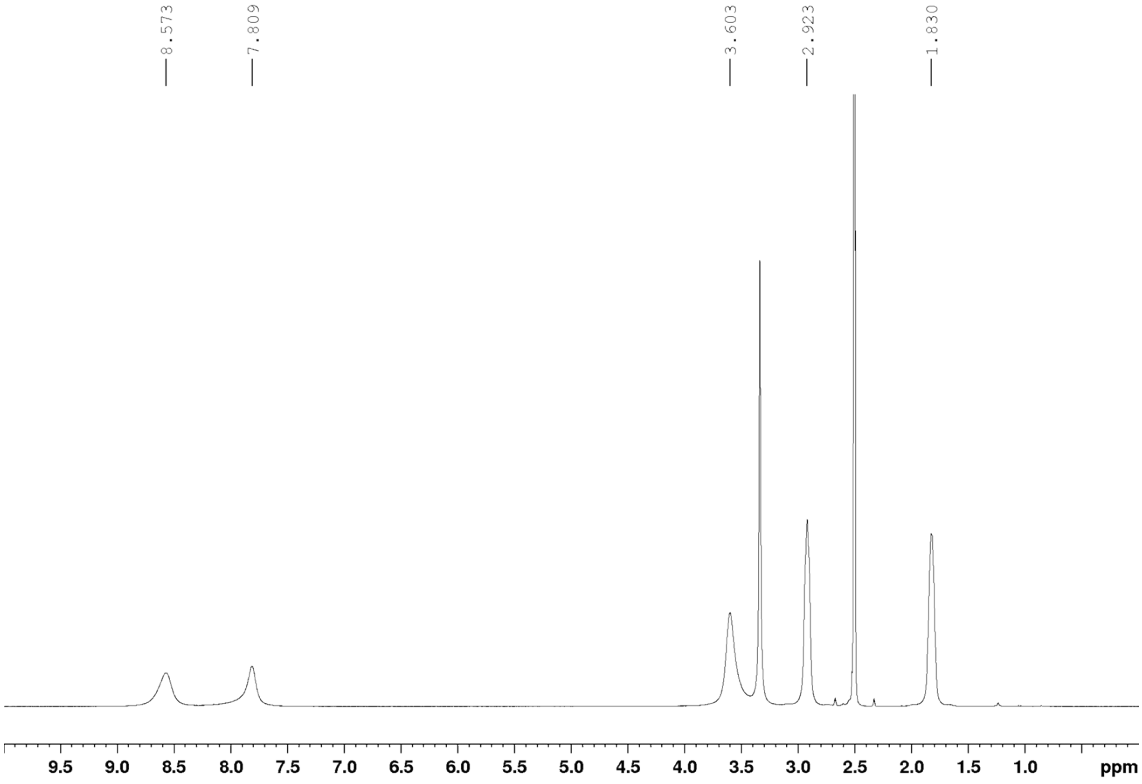

Figure S10. ^{1}H NMR spectrum of **L5·2CF_3COOH** in DMSO-d_6/0.5% water solution at 298 K.

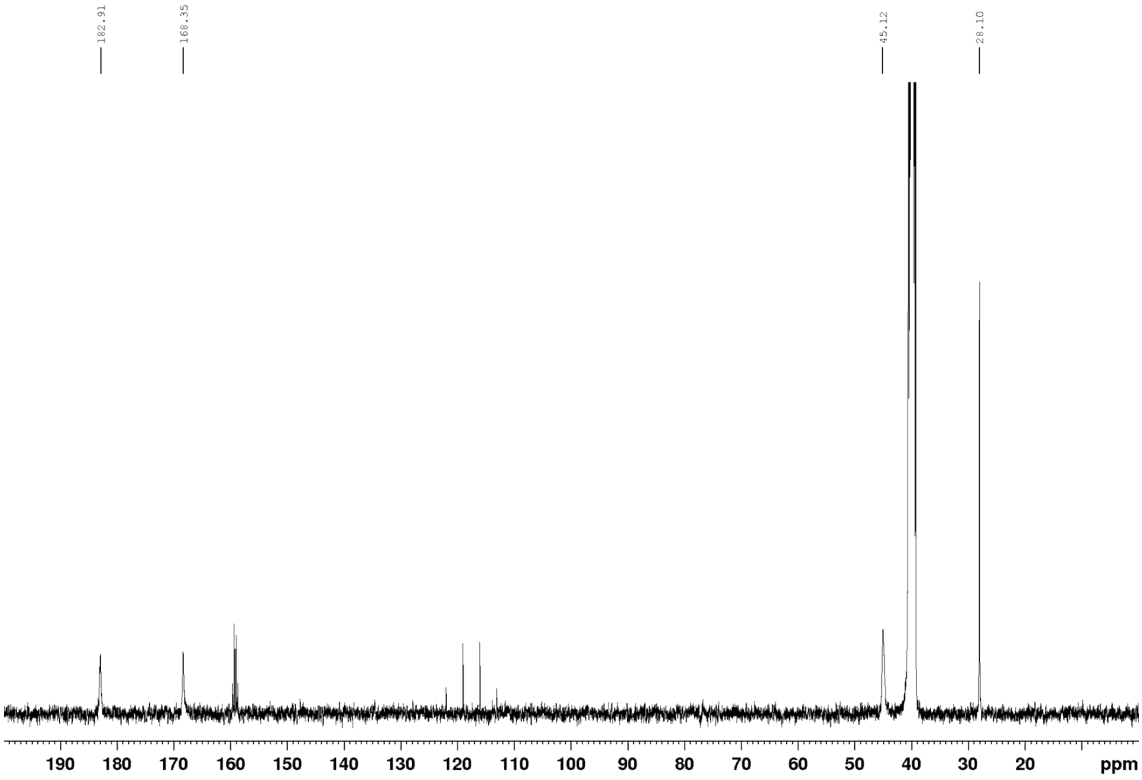

Figure S11. ^{13}C NMR spectrum of **L5·2CF$_3$COOH** in DMSO-d_6/0.5% water solution at 298 K.

4. Photophysical characterization

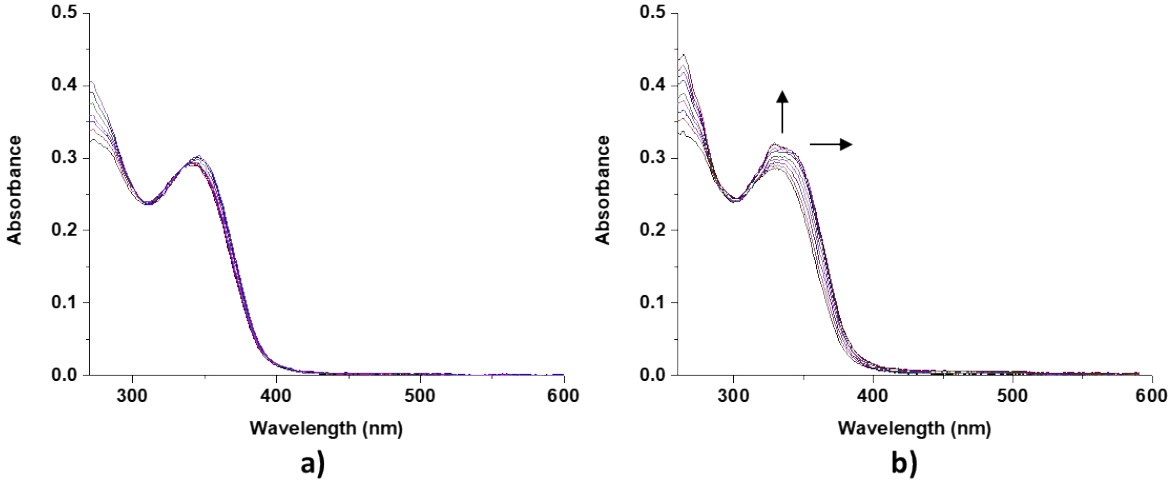

Figure S12. UV-Vis spectra for the titration in DMSO of **L4** ($1.1 \cdot 10^{-5}$ M) in the presence of increasing amount of a) KETNa ($2.0 \cdot 10^{-3}$M) and b) NPXNa ($1.9 \cdot 10^{-3}$ M).

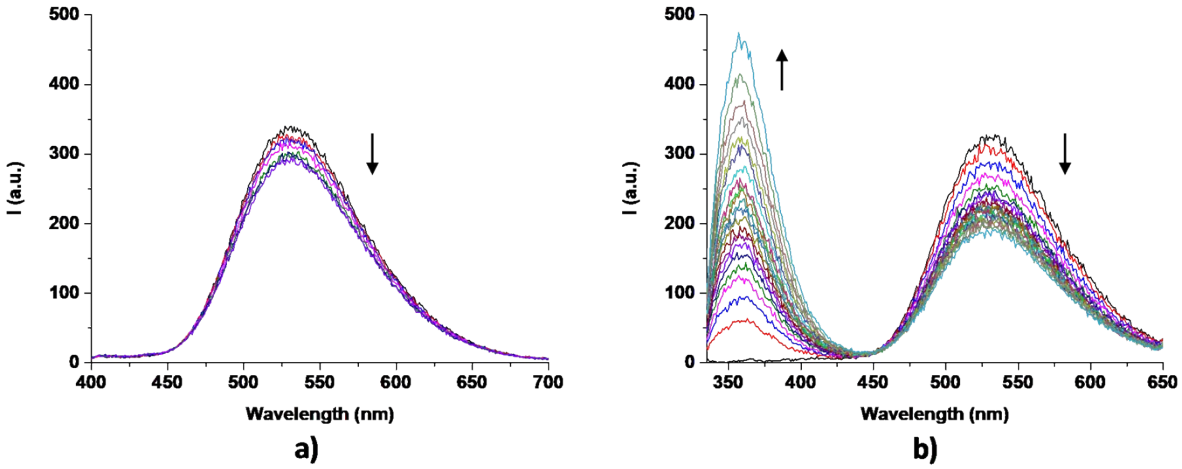

Figure S13. Emission spectra in DMSO of **L4** ($1.0 \cdot 10^{-5}$ M) in the presence of increasing amount of a) KETNa ($2.0 \cdot 10^{-3}$M) and b) NPXNa ($1.9 \cdot 10^{-3}$ M).

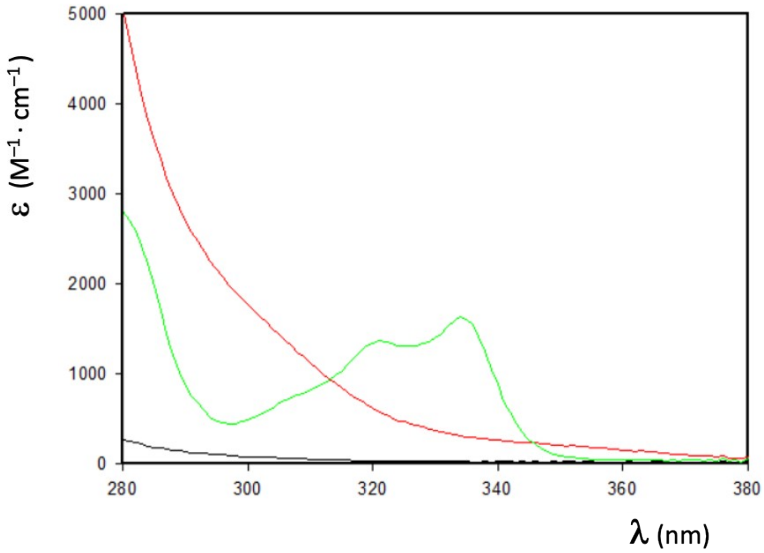

Figure S14. Absorption spectra in CH_3CN/DMSO 9/1 solution of naproxen (green line), ketoprofen (red line), and benzoate (black line) as their sodium salts.

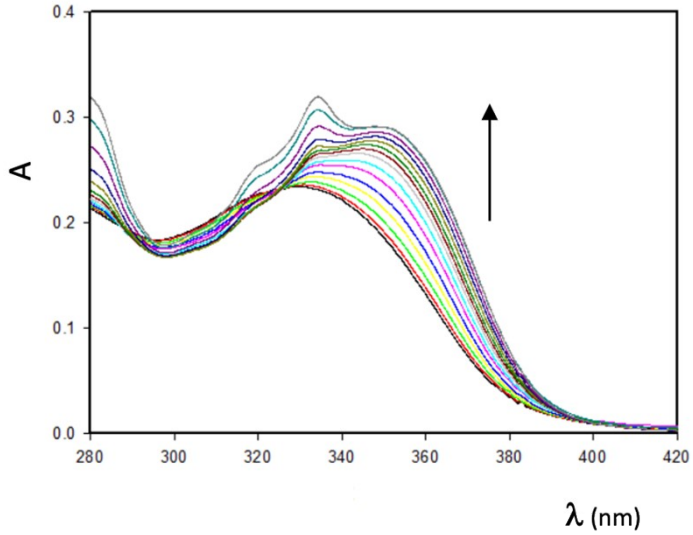

Figure S15. Absorption spectra in CH_3CN/DMSO 9/1 solution of **L4** (10 μM) upon addition of increasing amounts (0 – 5 equiv) of naproxen as its sodium salt.

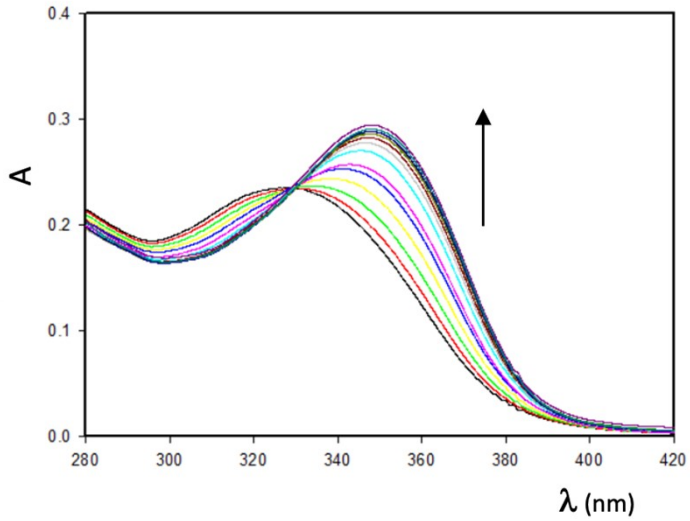

Figure S16. Absorption spectra in CH_3CN/DMSO 9/1 solution of **L4** (10 µM) upon addition of increasing amounts (0 – 5 equiv) of benzoate as its sodium salt.

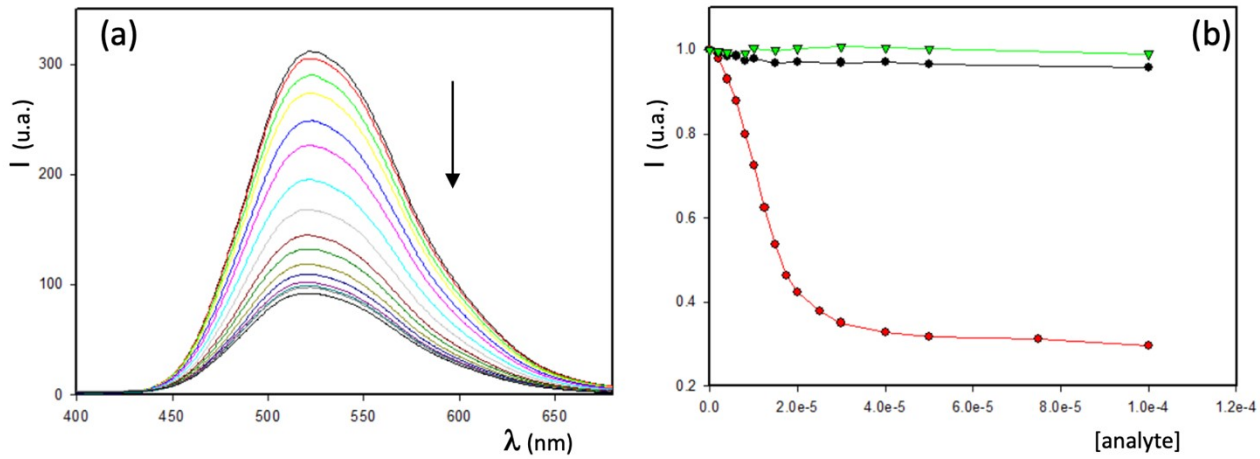

Figure S17. (a) Fluorescence spectra (λ_{exc} = 350 nm) in CH_3CN/DMSO 9/1 solution of **L2** (10 µM) upon addition of increasing amount of ketoprofen; (b) normalized fluorescence intensity of **L2** (λ_{exc} = 350 nm; λ_{em} = 525 nm) upon addition of increasing amount of ketoprofen (red circles), naproxen (green triangles), and benzoate (black circles) as their sodium salts.

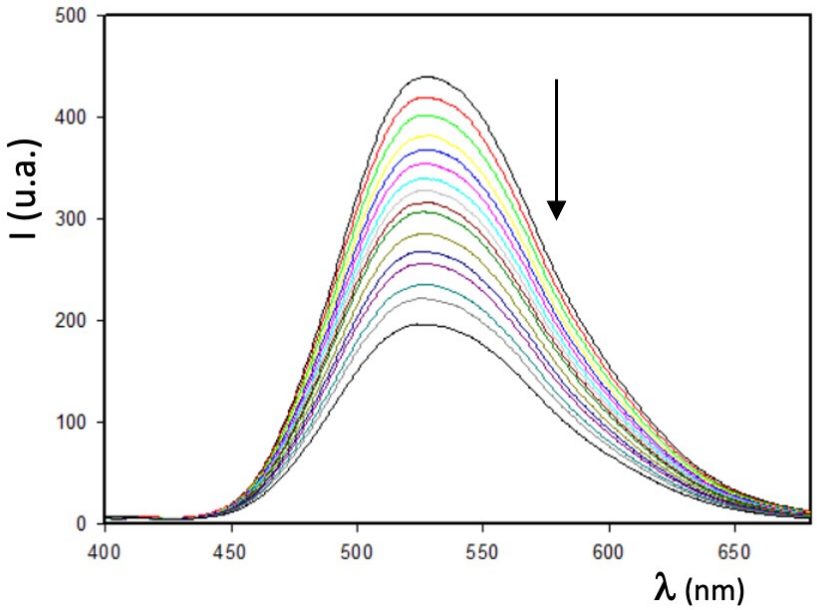

Figure S18. Fluorescence spectra (λ_{exc} = 350 nm) in CH_3CN/DMSO 9/1 solution of **L3** (10 µM) upon addition of increasing amount of ketoprofen.

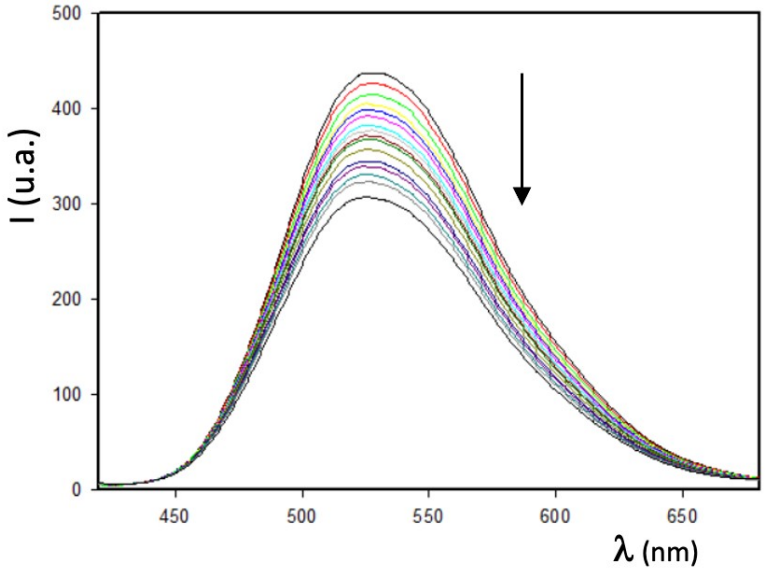

Figure S19. Fluorescence spectra (λ_{exc} = 350 nm) in CH_3CN/DMSO 9/1 solution of **L3** (10 µM) upon addition of increasing amount of naproxen.

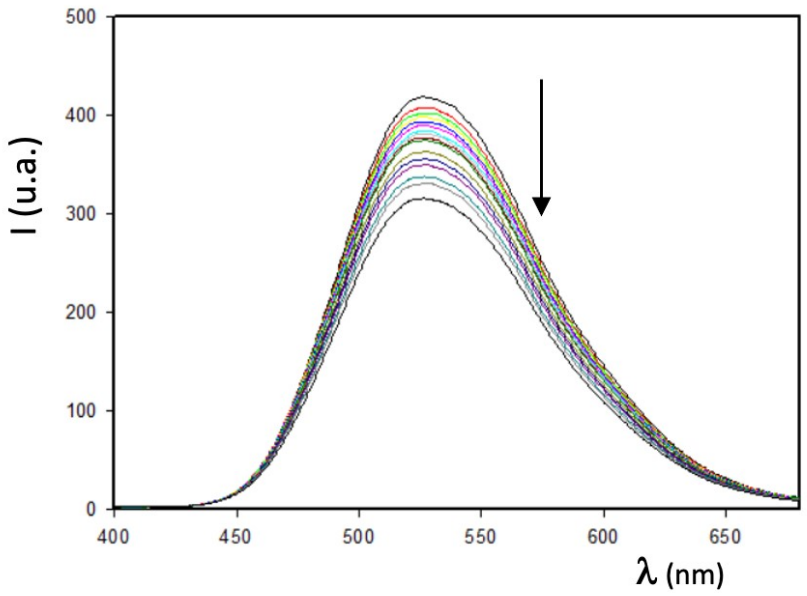

Figure S20. Fluorescence spectra (λ_{exc} = 350 nm) in CH_3CN/DMSO 9/1 solution of **L3** (10 µM) upon addition of increasing amount of benzoate.

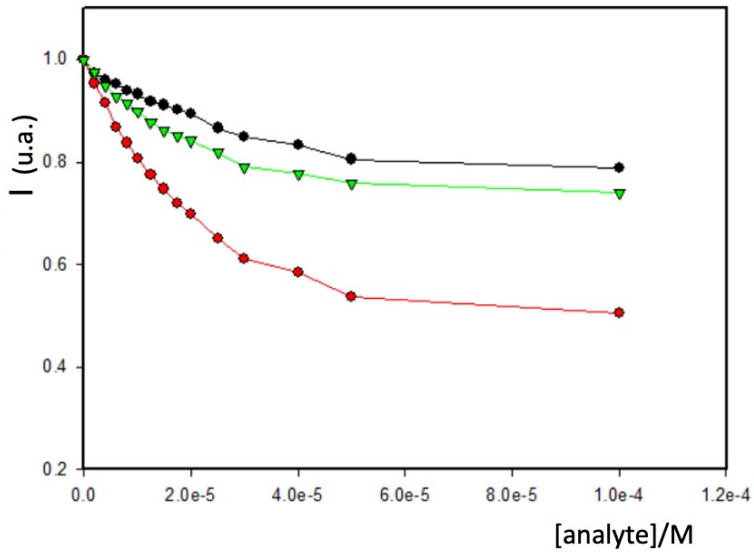

Figure S21. Normalized fluorescence intensity (λ_{exc} = 350 nm; λ_{em} = 525 nm) of **L3** (10 µM) upon addition of increasing amount of ketoprofen (red circles), naproxen (green triangles), and benzoate (black circles).

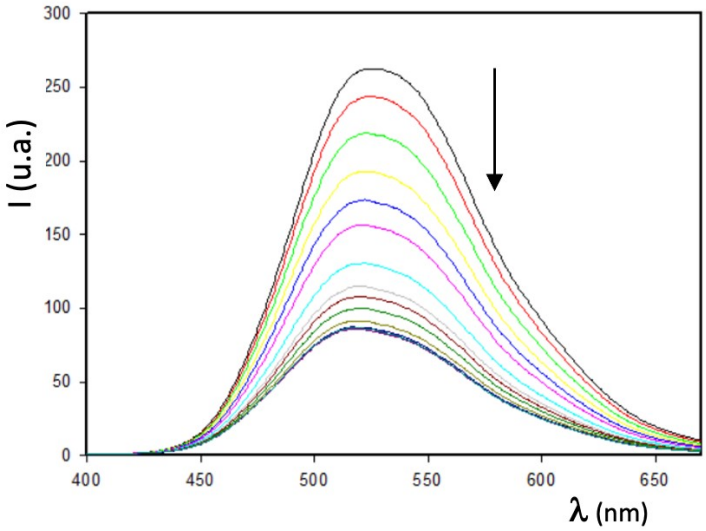

Figure S22. Fluorescence spectra (λ_{exc} = 350 nm) in CH_3CN/DMSO 9/1 solution of **L4** (10 µM) upon addition of increasing amount of ketoprofen.

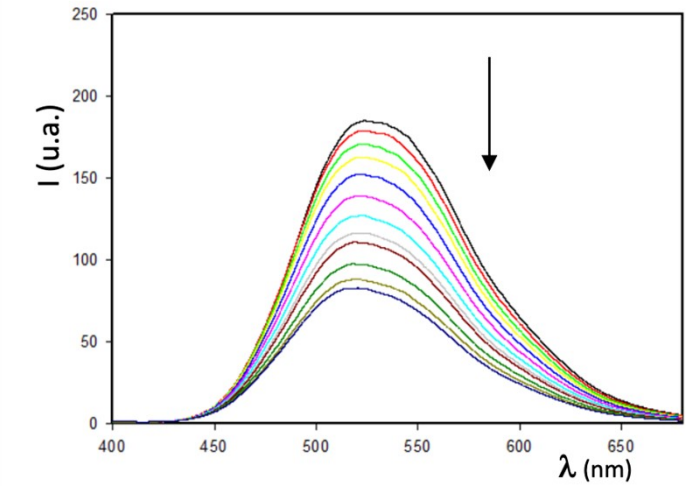

Figure S23. Fluorescence spectra (λ_{exc} = 350 nm) in CH_3CN/DMSO 9/1 solution of **L4** (10 µM) upon addition of increasing amount of naproxen.

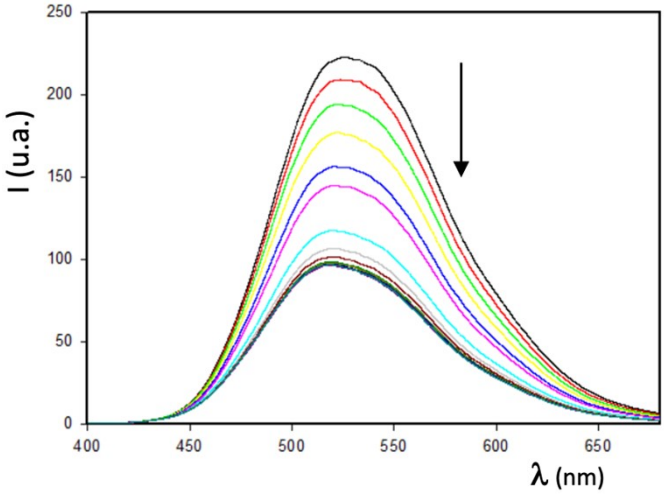

Figure S24. Fluorescence spectra (λ_{exc} = 350 nm) in CH_3CN/DMSO 9/1 solution of **L4** (10 µM) upon addition of increasing amount of benzoate.

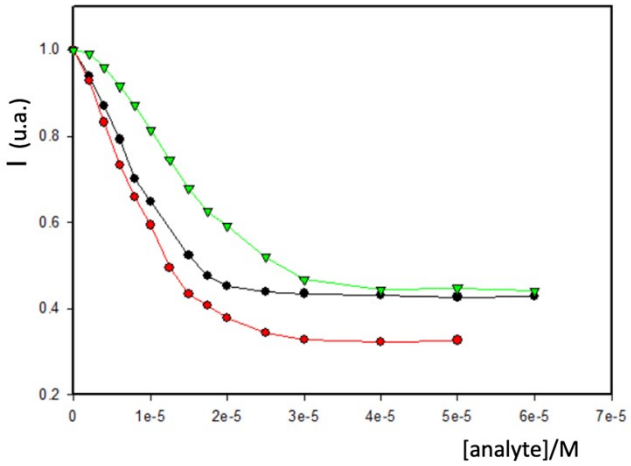

Figure S25. Normalized fluorescence intensity (λ_{exc} = 350 nm; λ_{em} = 525 nm) of **L4** (10 µM) upon addition of increasing amount of ketoprofen (red circles), naproxen (green triangles), and benzoate (black circles).

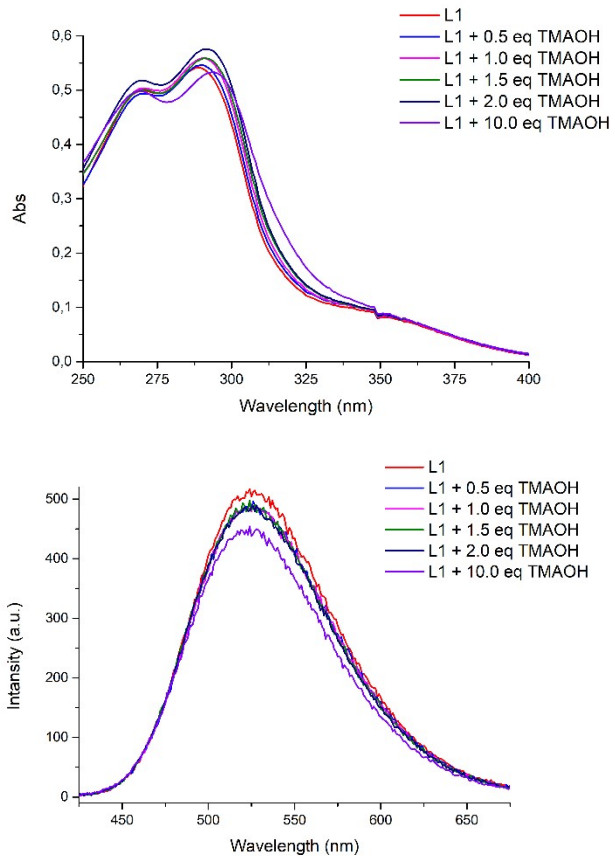

A) **B)**

Figure S26. Absorption and fluorescence spectra (λ_{exc} = 350 nm) in CH_3CN/DMSO 9/1 solution of **L1** (10 µM) upon addition of increasing amount of TMAOH.

4. ^{1}H-NMR titration studies

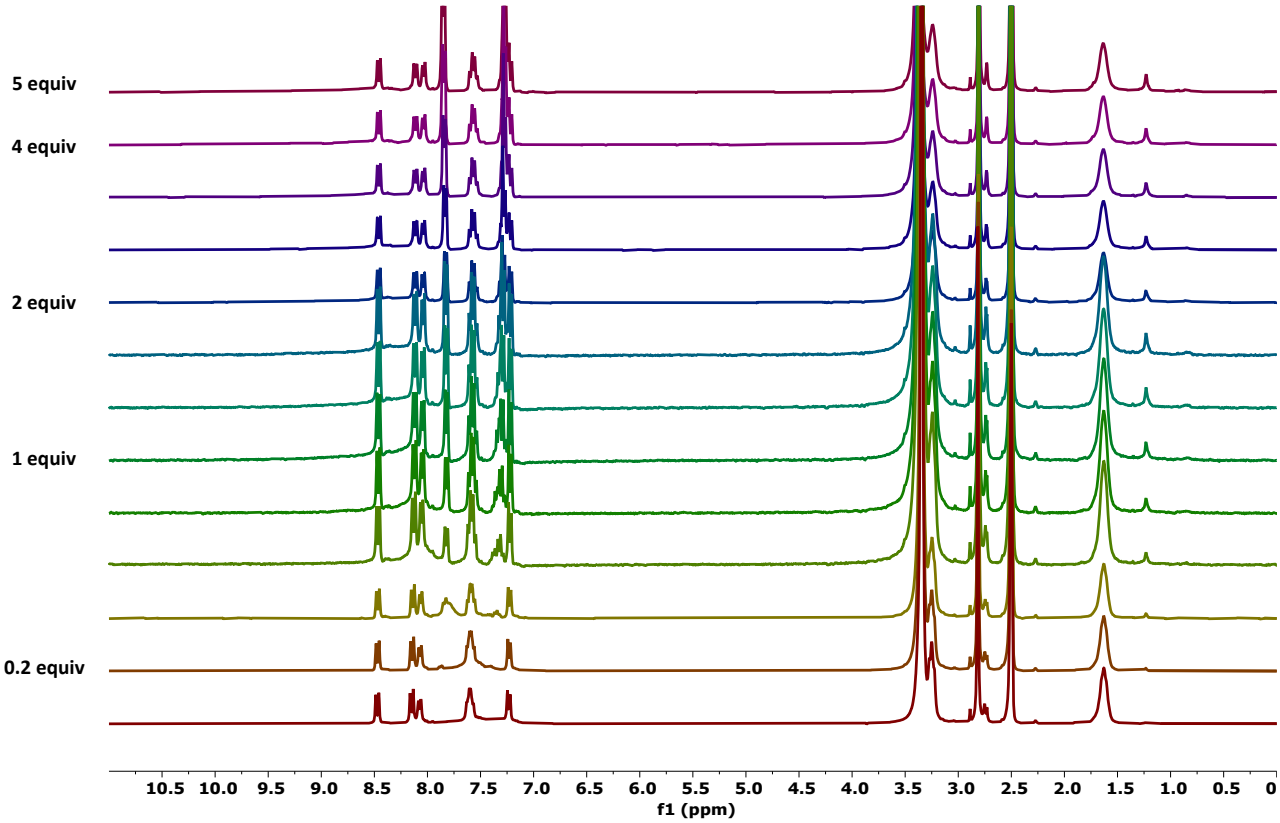

Figure S27. Stack-plot of the ^{1}H NMR titration of **L1** ($5.0 \cdot 10^{-3}$ M) with NaBzO (0.075 M) in DMSO-d_6/0.5% water.

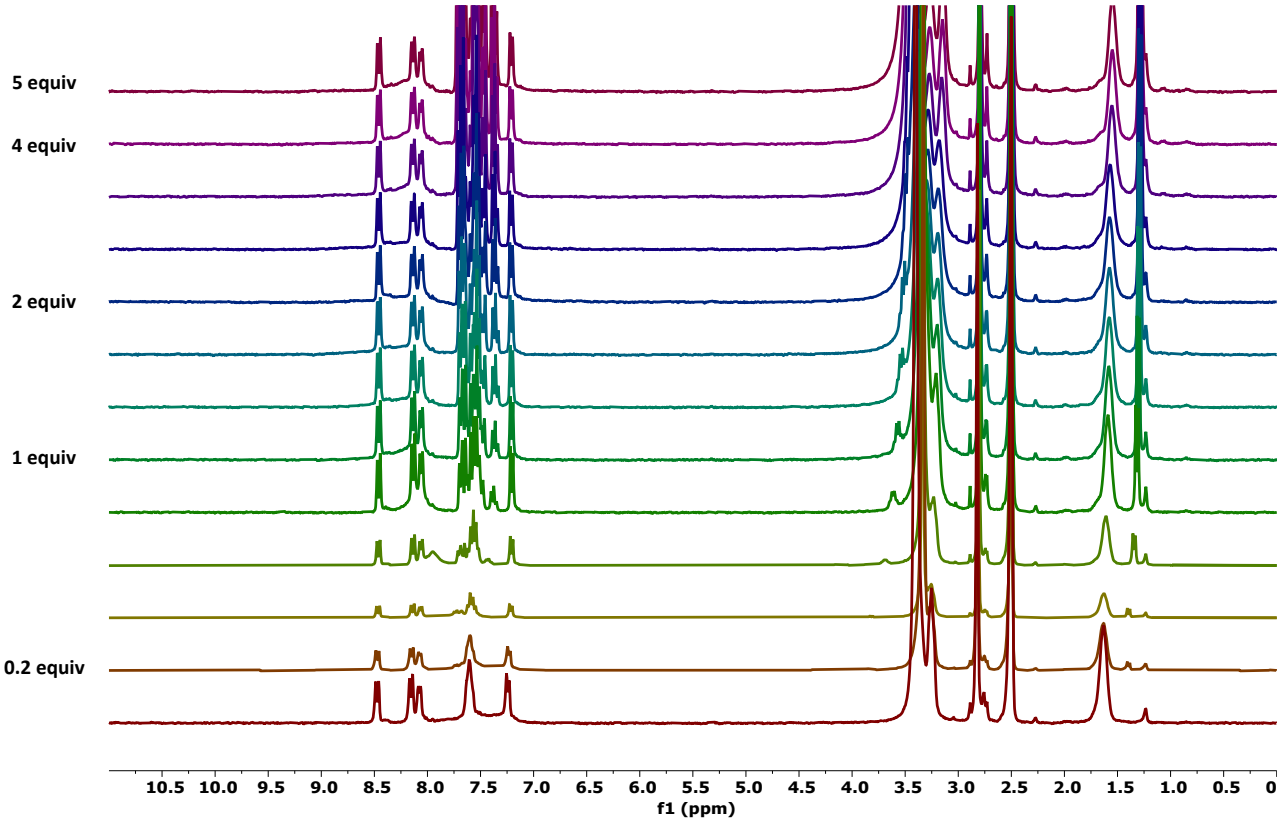

Figure S28. Stack-plot of the ^{1}H NMR titration of **L1** ($5.0 \cdot 10^{-3}$ M) with NaKET (0.075 M) in DMSO-d_6/0.5% water

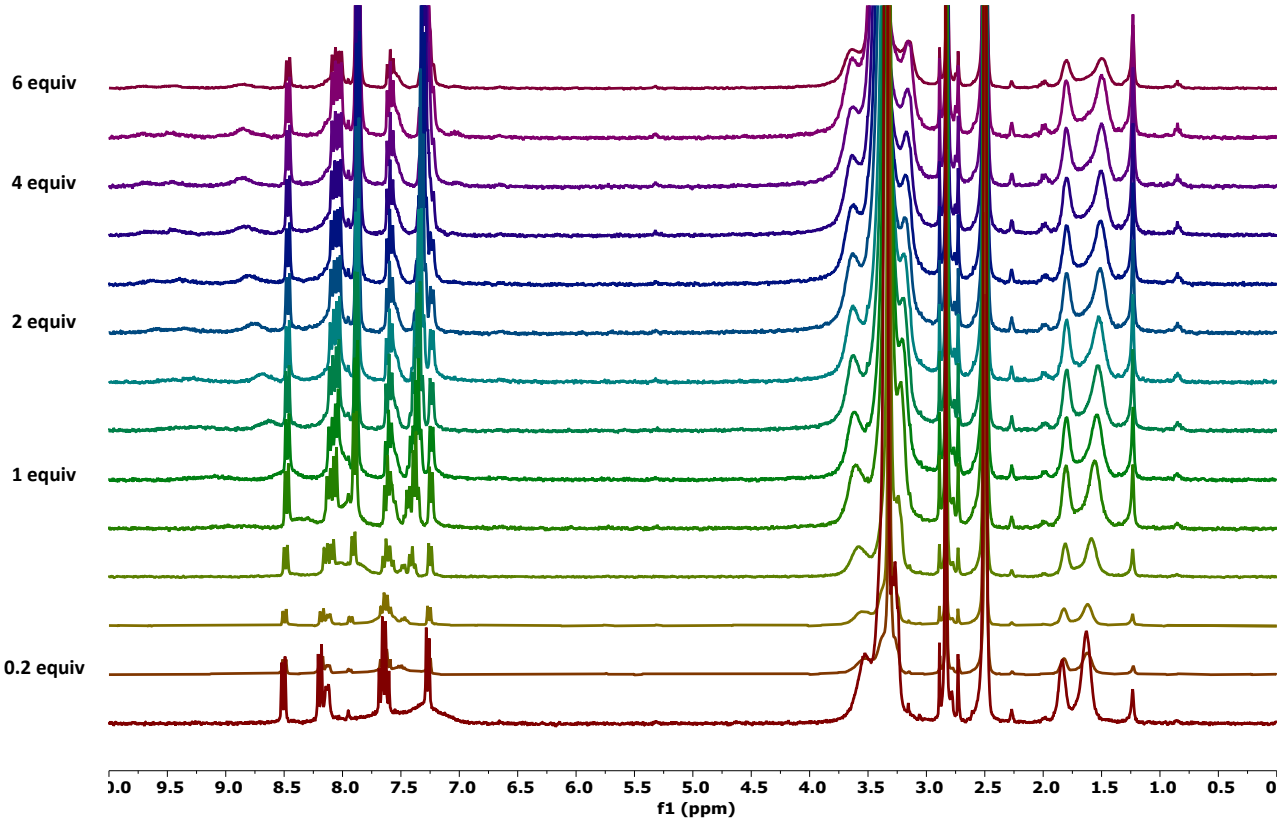

Figure S29. Stack-plot of the ^{1}H NMR titration of **L2** ($5.0 \cdot 10^{-3}$ M) with NaBzO (0.075 M) in DMSO-d_6/0.5% water.

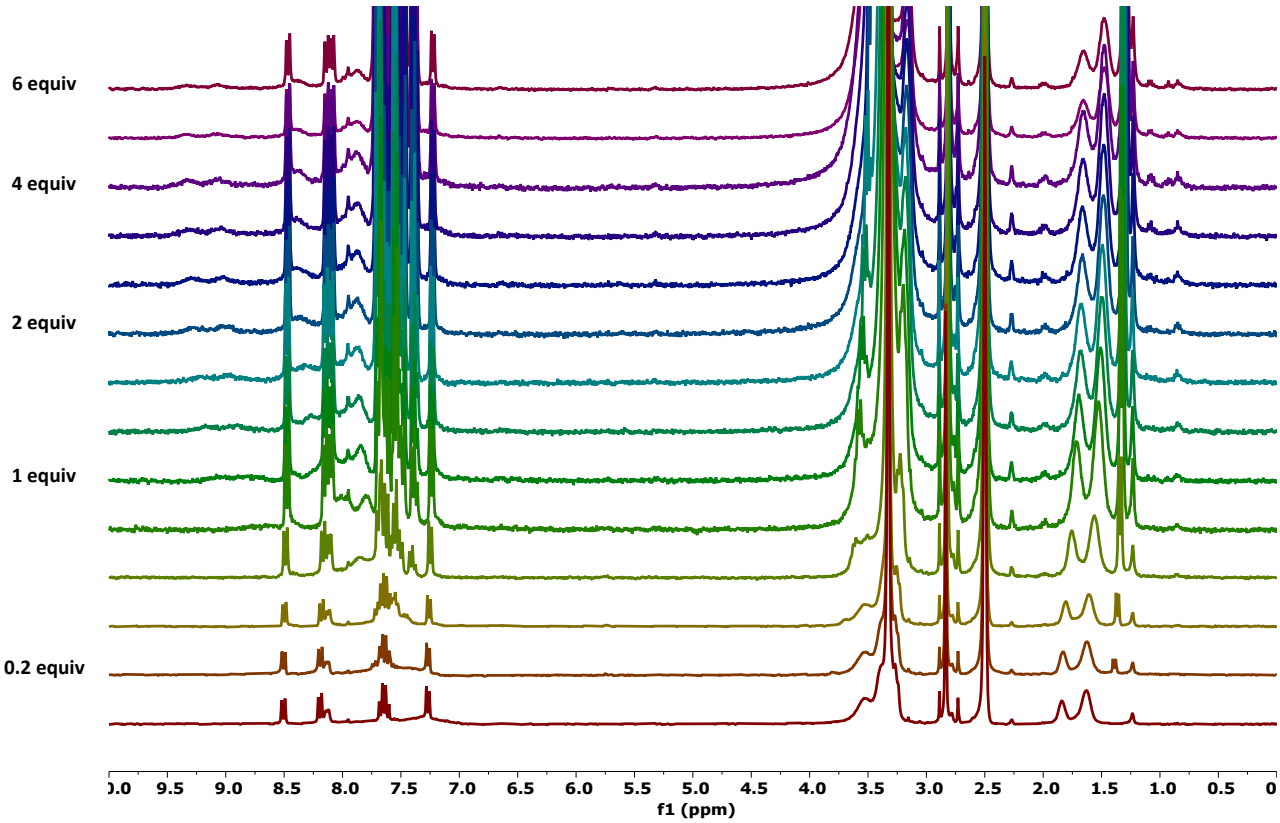

Figure S30. Stack-plot of the ^{1}H NMR titration of **L2** ($5.0 \cdot 10^{-3}$ M) with NaKET (0.075 M) in DMSO d_6/0.5% water.

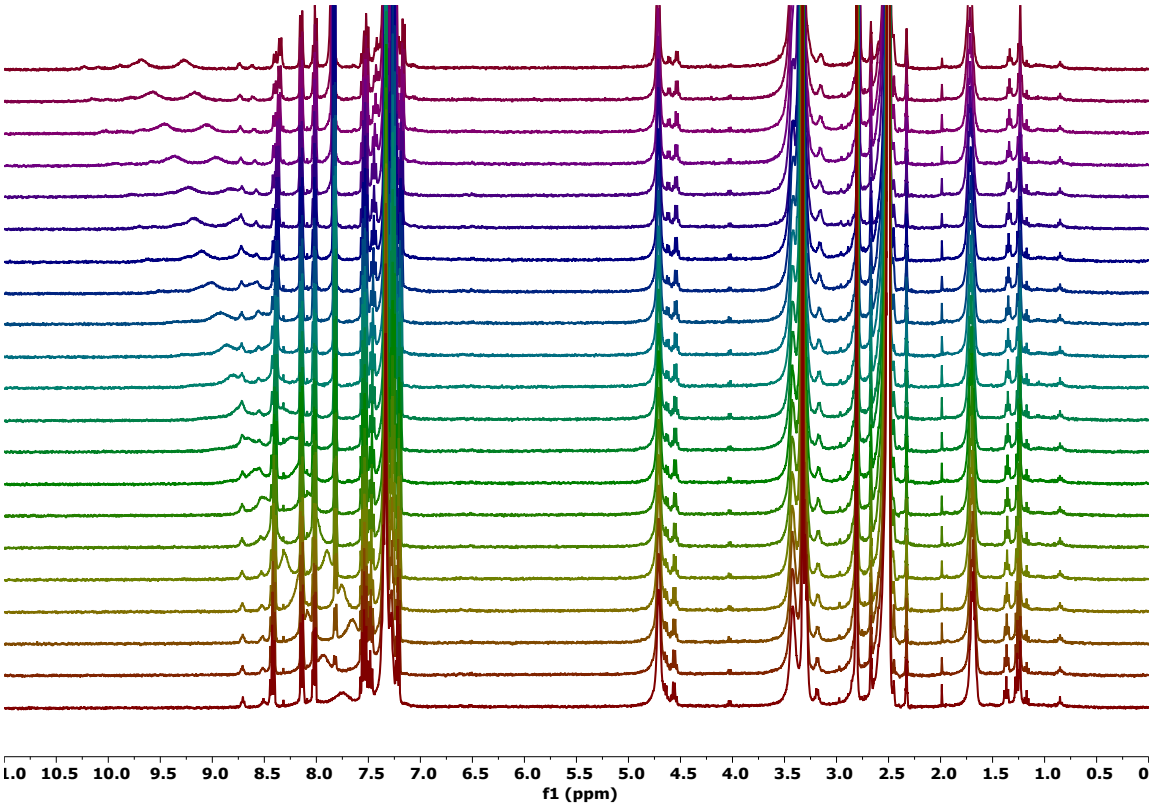

(A)

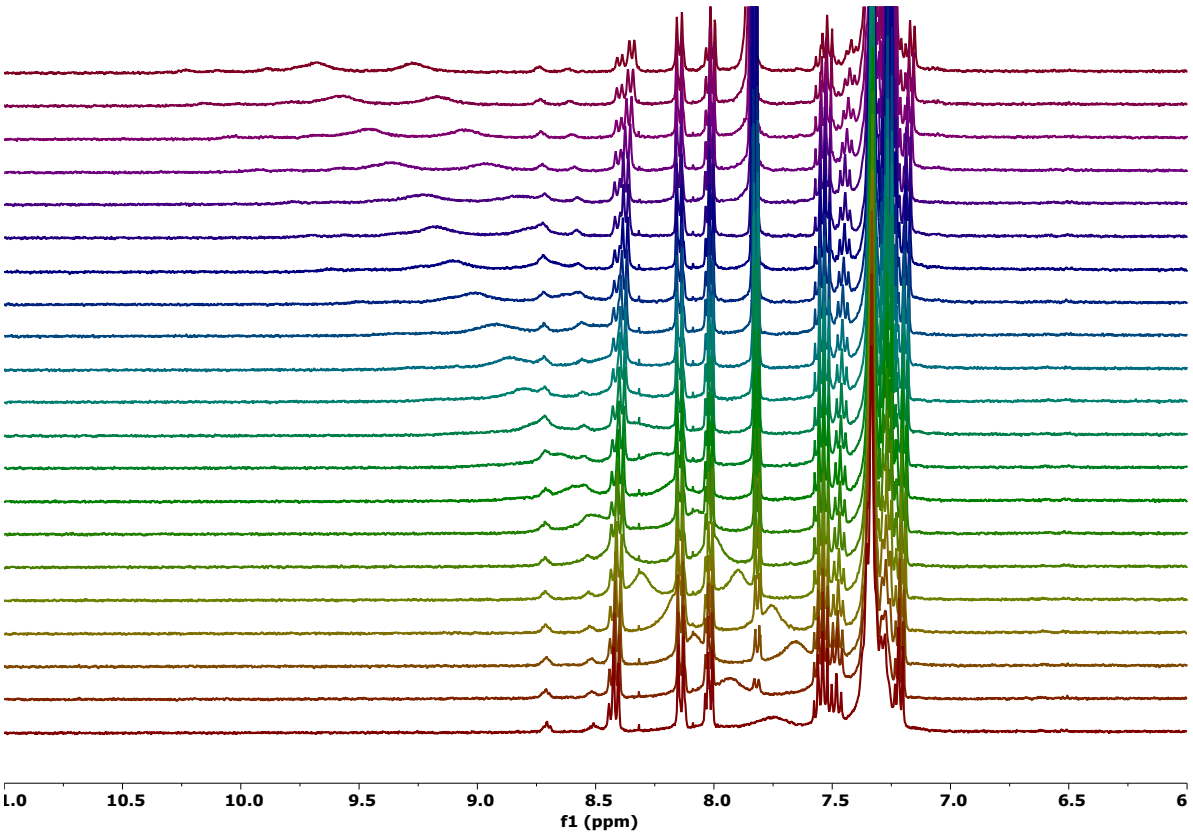

(B)

Figure S31. Stack-plot of the ^{1}H NMR titration of **L3** ($5.0 \cdot 10^{-3}$ M) with NaBzO 0.075M) in DMSO-d_6/0.5% water solution(A); zoom of the aromatic region (B).

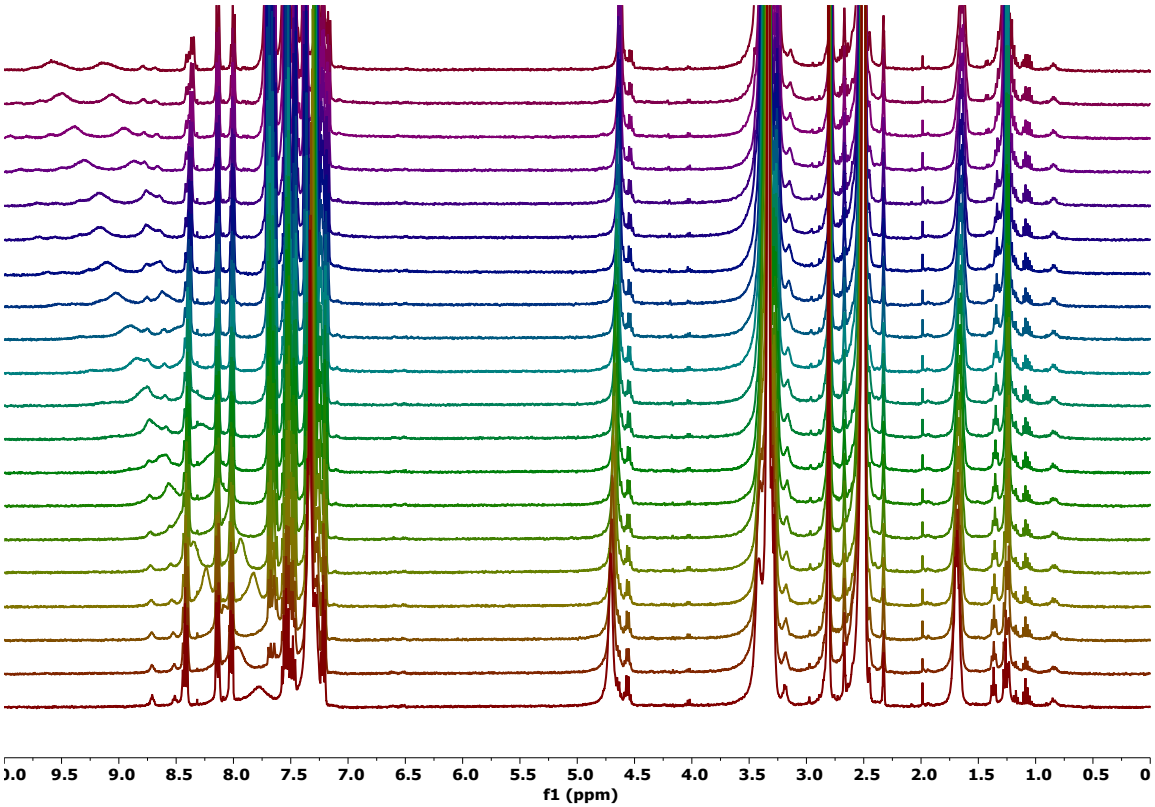

(A)

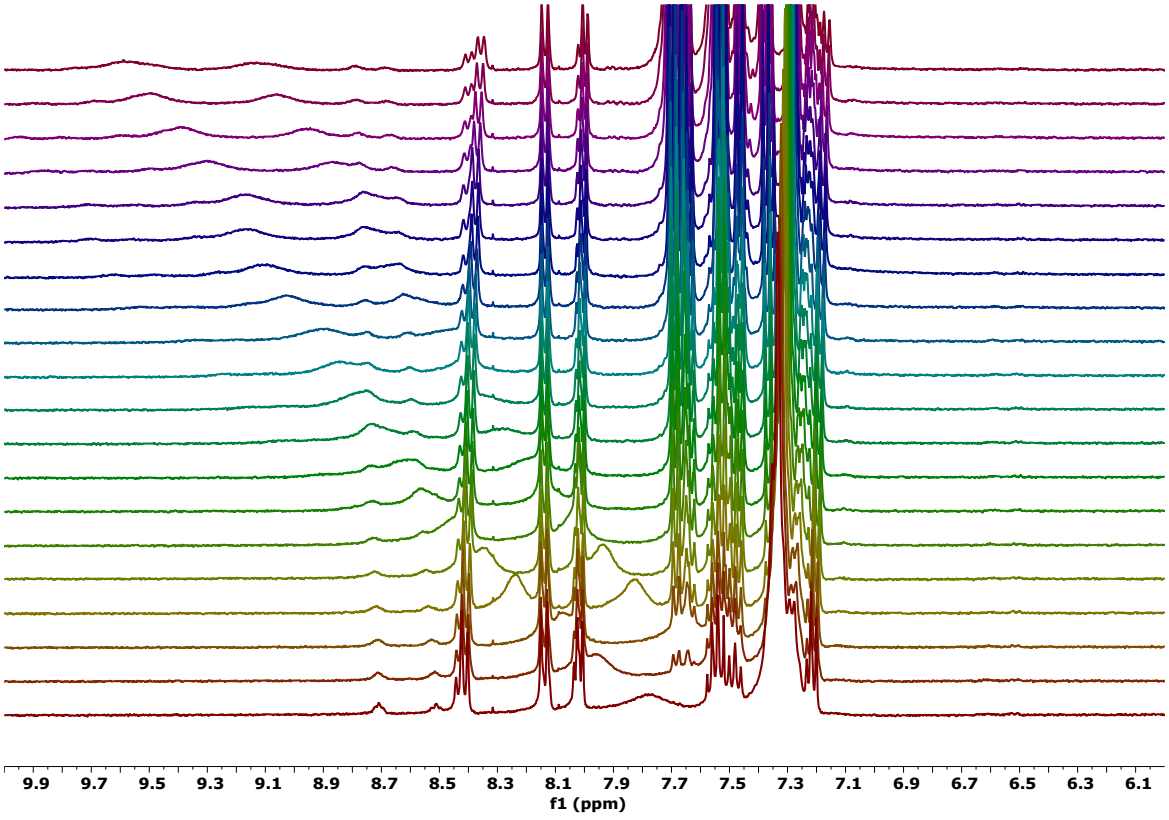

(B)

Figure S32. Stack-plot of the ^{1}H NMR titration of **L3** (0.005 M) with NaKET (0.075 M) in DMSO-d_6/0.5% water solution(A); zoom of the aromatic region (B).

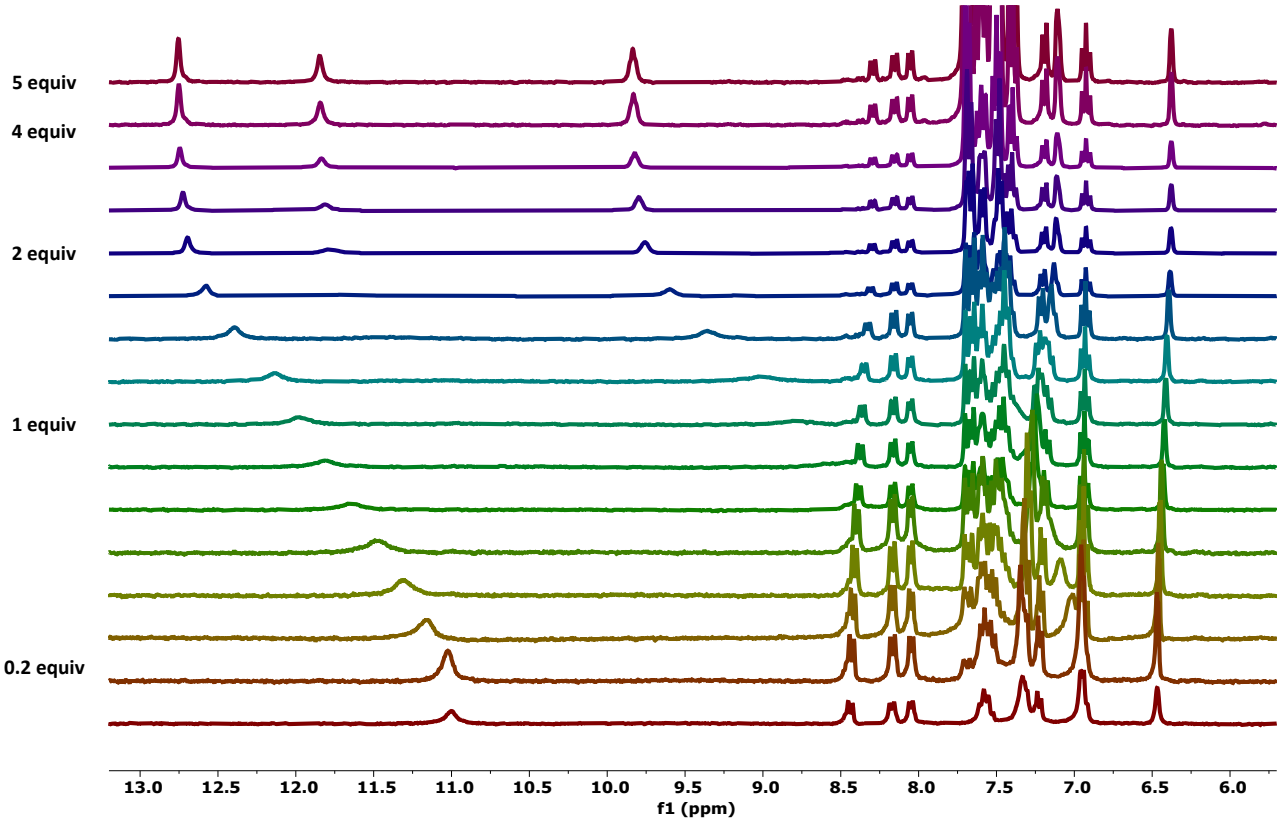

http://app.supramolecular.org/bindfit/view/907a3966-fd91-4cea-9b65-4912c96878c5

Figure S33. ^{1}H NMR titration of **L4** (0.005 M) with NaKET (0.075 M) in DMSO-d_6/0.5% water

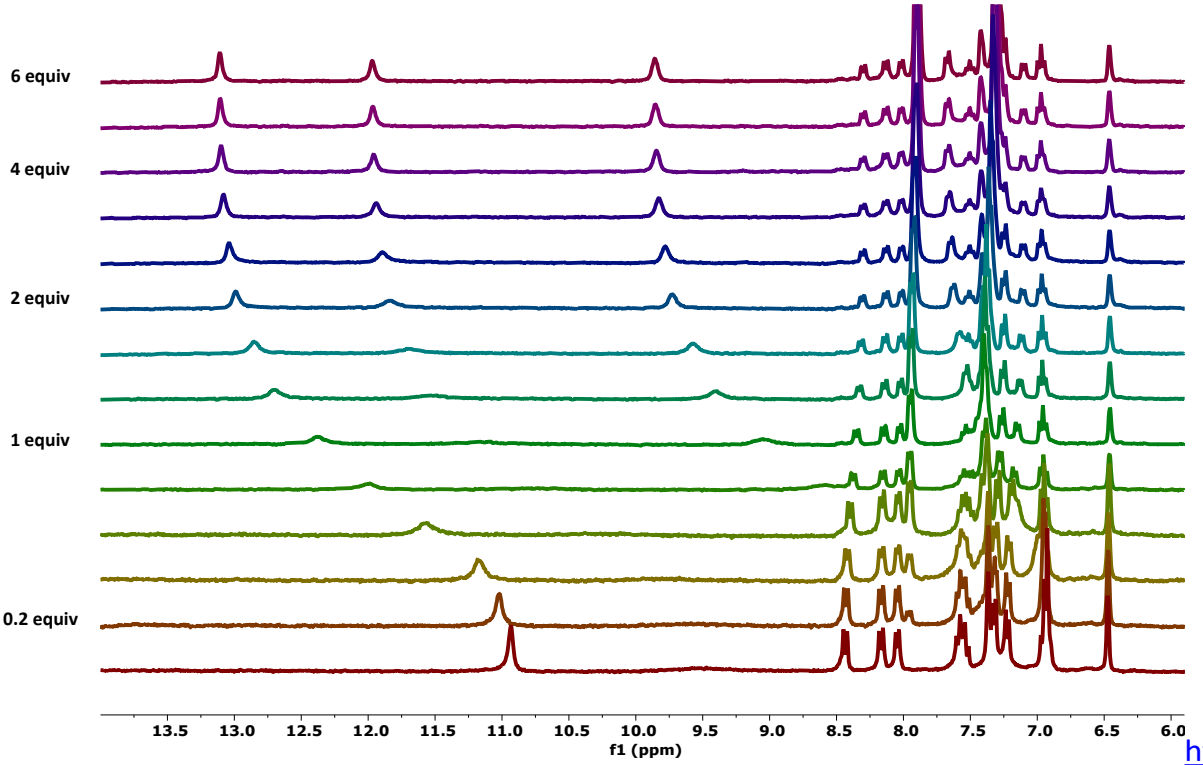

http://app.supramolecular.org/bindfit/view/c77c8bdc-2962-421d-8ce0-6c431eaa7850

Figure S34. ^{1}H NMR titration of **L4** (0.005 M) with NaBzO (0.075 M) in DMSO-d_6/0.5% water

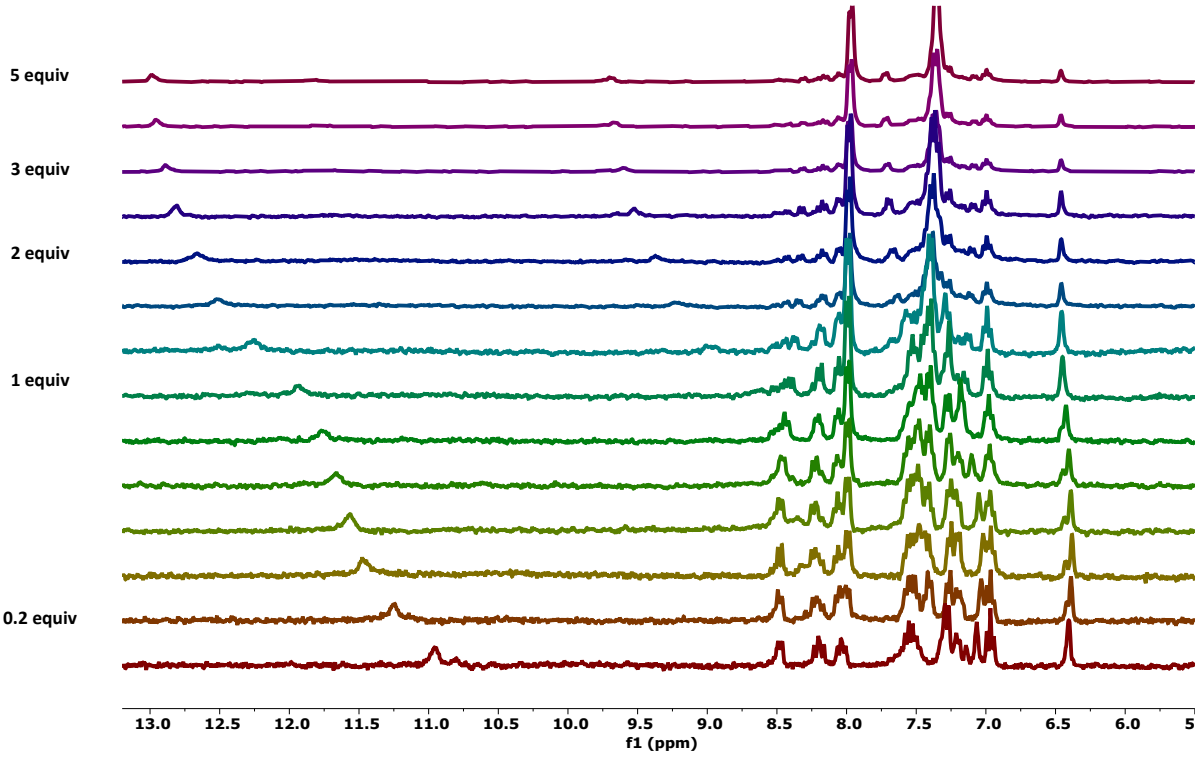

http://app.supramolecular.org/bindfit/view/106bf2f1-a6b9-4379-bc48-2bbb65f0ef71

Figure S35. ^{1}H NMR titration of **L4** (0.001 M) with NaBzO (0.075 M) in CD_3CN-d_3/DMSO-d_6

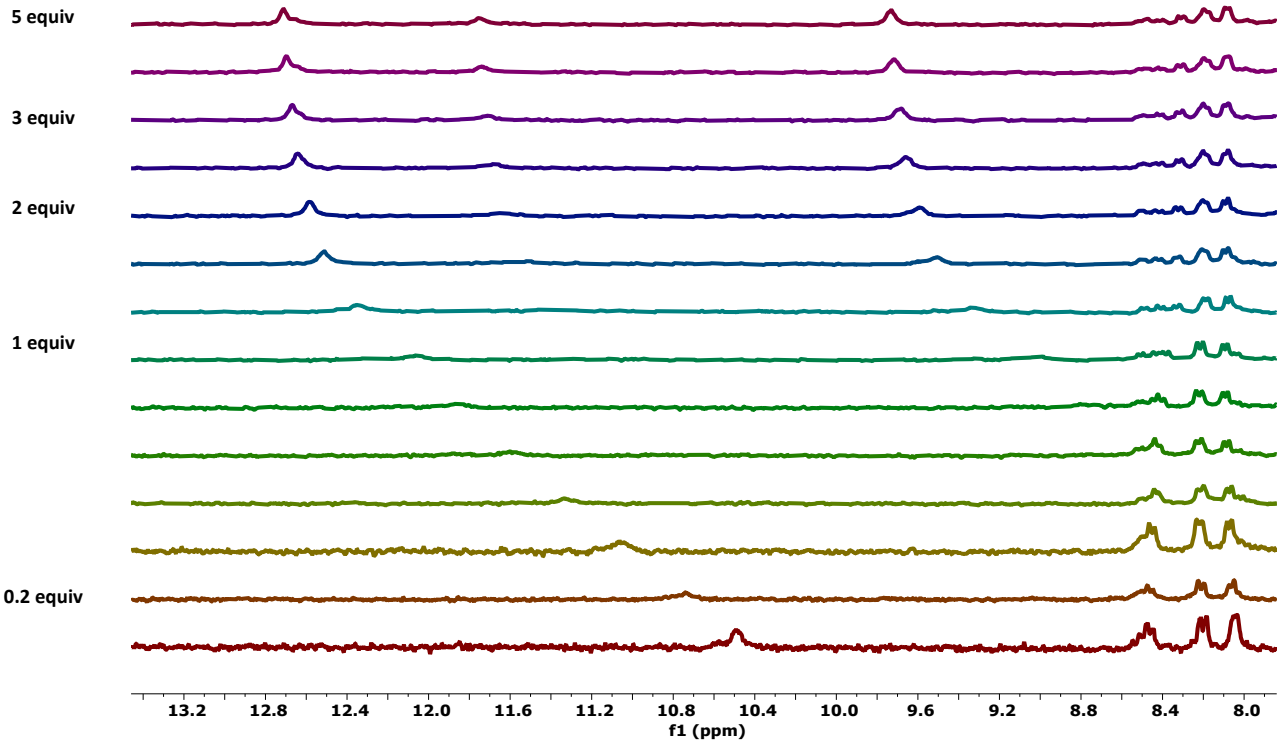

http://app.supramolecular.org/bindfit/view/5c5d3e7a-86f9-40b7-af05-f3ae4ddb8092

Figure S36. ^{1}H NMR titration of **L4** (0.001 M) with NaKeto (0.075 M) in CD_3CN-d_3/DMSO-d_6

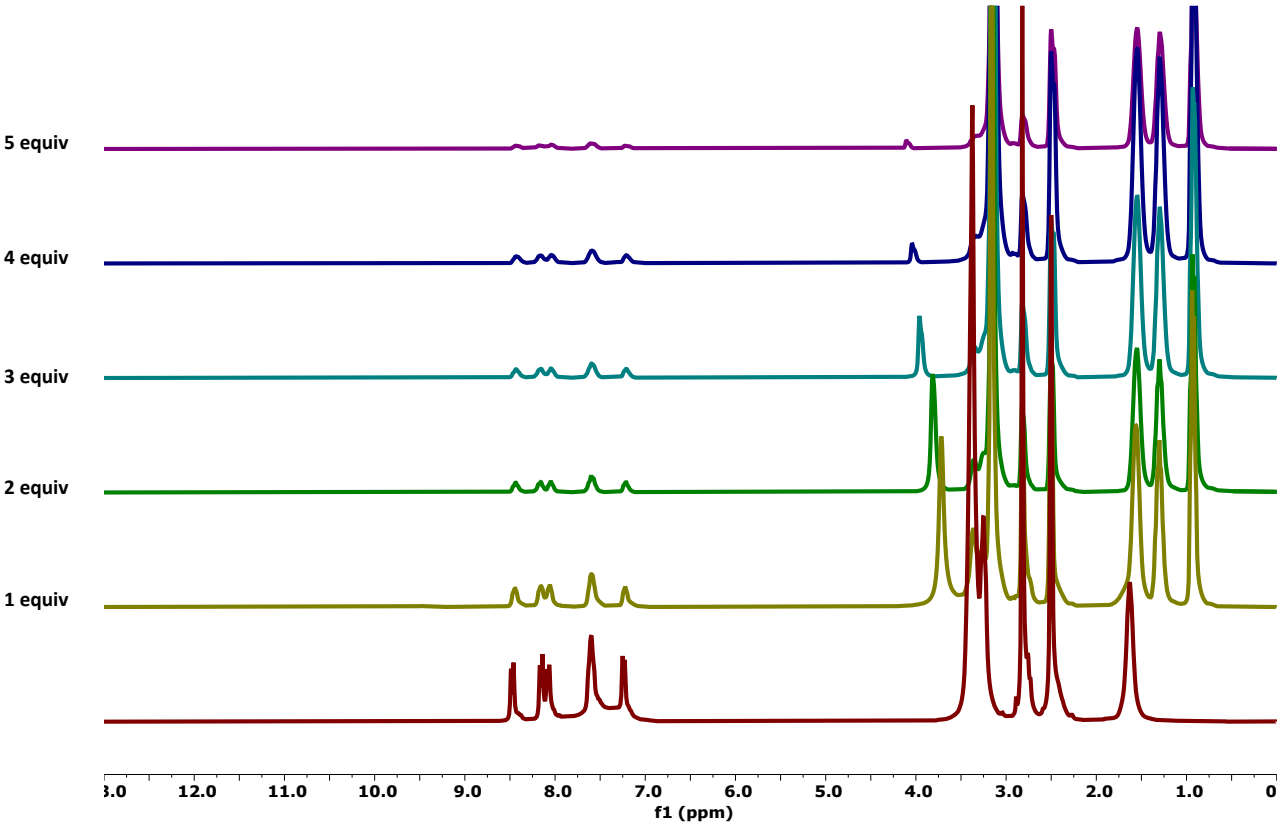

Figure S37. ^{1}H NMR titration of **L1** (0.005 M) with TBAOH(0.075 M) in DMSO-d_6/0.5% water

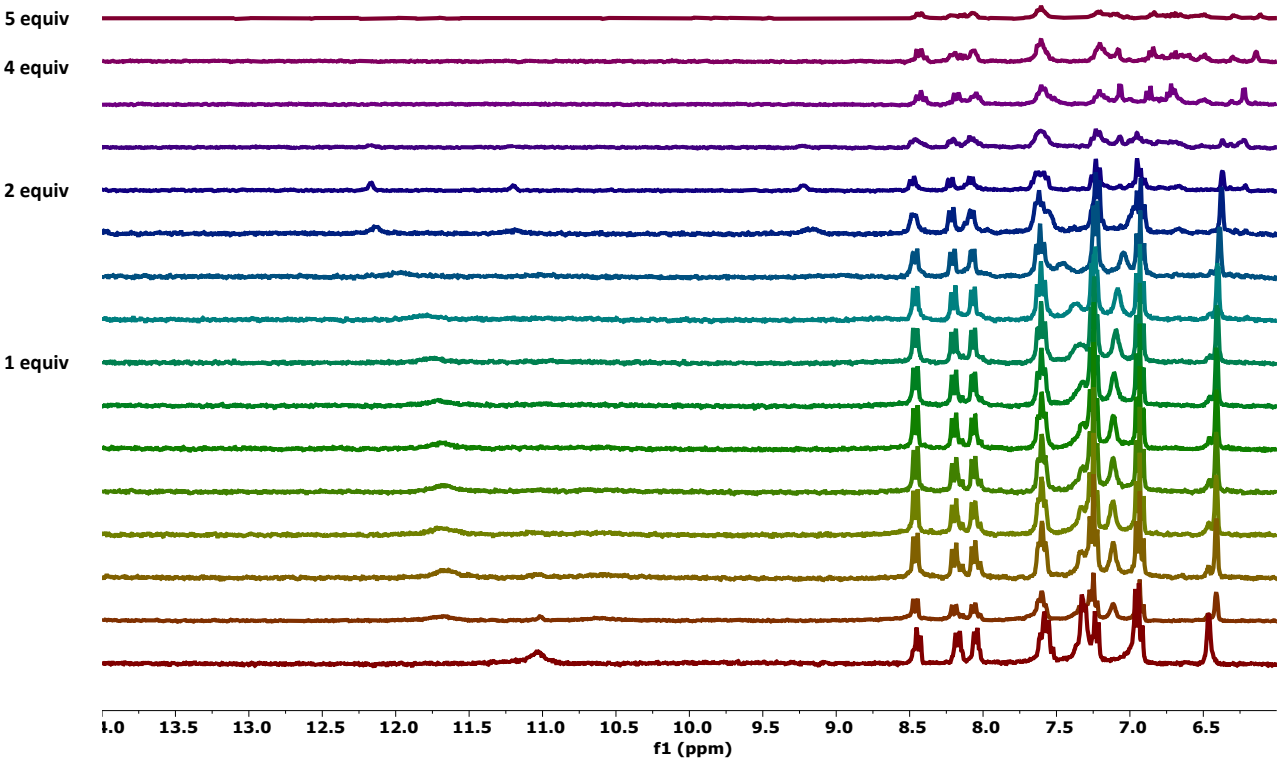

Figure S38. ^{1}H NMR titration of **L4** ($5.0 \cdot 10^{-3}$ M) with TBAOH (0.075 M) in DMSO-d_6/0.5% water.

Table S1. Association constant for the formation of the 1:2 host-guest adducts (in DMSO-d_6/0.5% water) and for the 1:1 host-guest adducts (in CD_3CN-d_3/DMSO-d_6) of **L4** following the downfield shift of the signals attributed to the indole NHs and the squaramide NHs adjacent to the alkyl chain. All the errors are <12%.

	K_{ass} /(mol/L)$^{-1}$	
Anion species		
KETNa	**BzONa**	**TBABzO**
DMSO-d_6/0.5% water		
	Stoichiometry 1:2	
$>10^4$	$>10^4$	$>10^4$
CD_3CN-d_3/DMSO-d_6 9:1 v/v		
	Stoichiometry 1:1	
4000	1250	//////

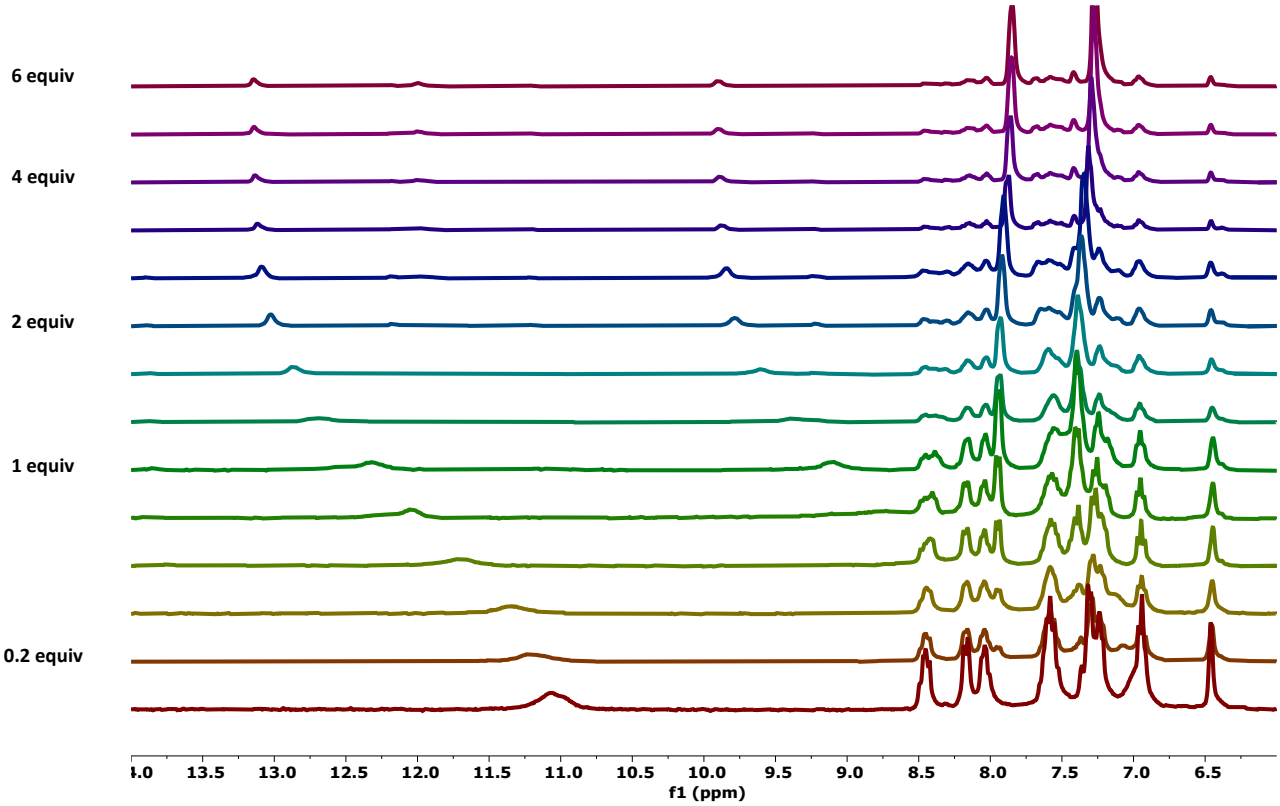

Figure S39. ^{1}H NMR titration of **L4** (0.005 M) with TBABzO (0.075 M) in DMSO-d_6/0.5% water

5. Theoretical calculations

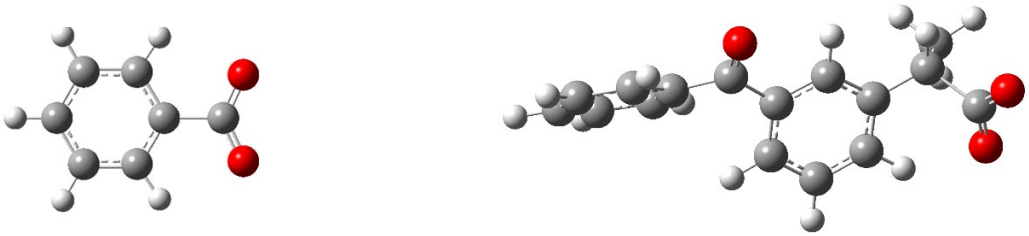

Figure S40. Benzoate (BzO^-; left) and ketoprofenate (KET^-; right) anions at the DFT-optimized geometries (carbon, grey; oxygen, red; hydrogen, white).

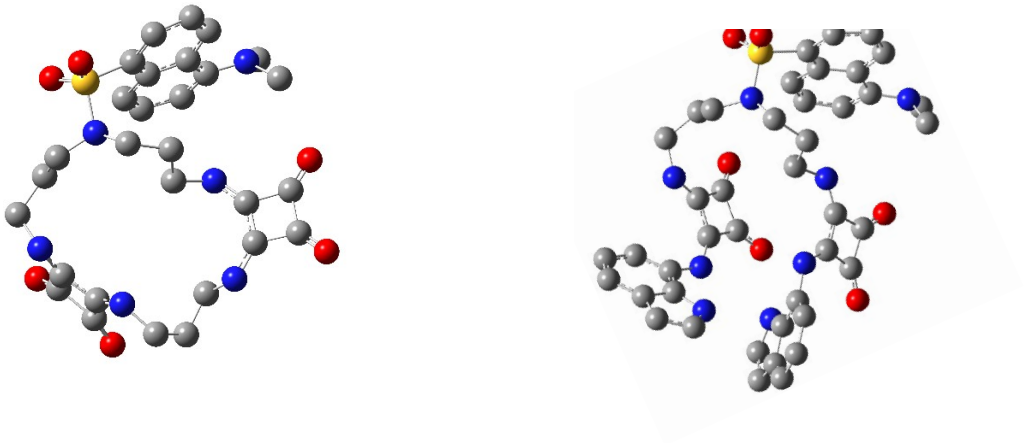

Figure S41. Compounds **L2** and **L4** at the DFT-optimized geometries (carbon, grey; oxygen, red; hydrogen, white; nitrogen, blue; sulfur, yellow).

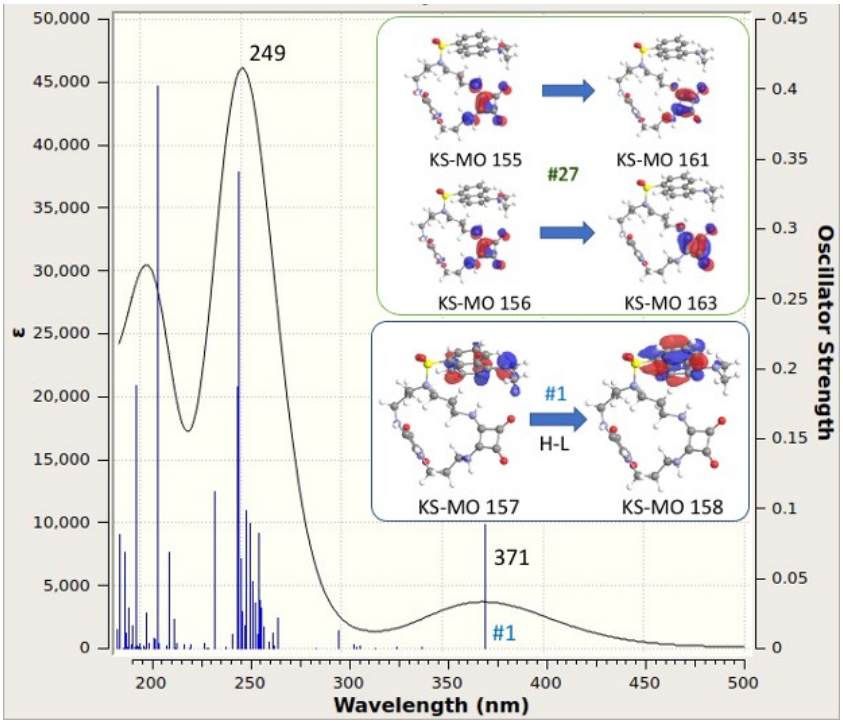

Figure S42. UV-Vis spectrum (250–500 nm) simulated for **L2** based on TD-DFT calculations. In the insets, the Kohn-Sham molecular orbitals (KS-MO) involved in the main monoelectronic transitions contributing to the GS⟶ES #1 and GS → ES #27 are represented.

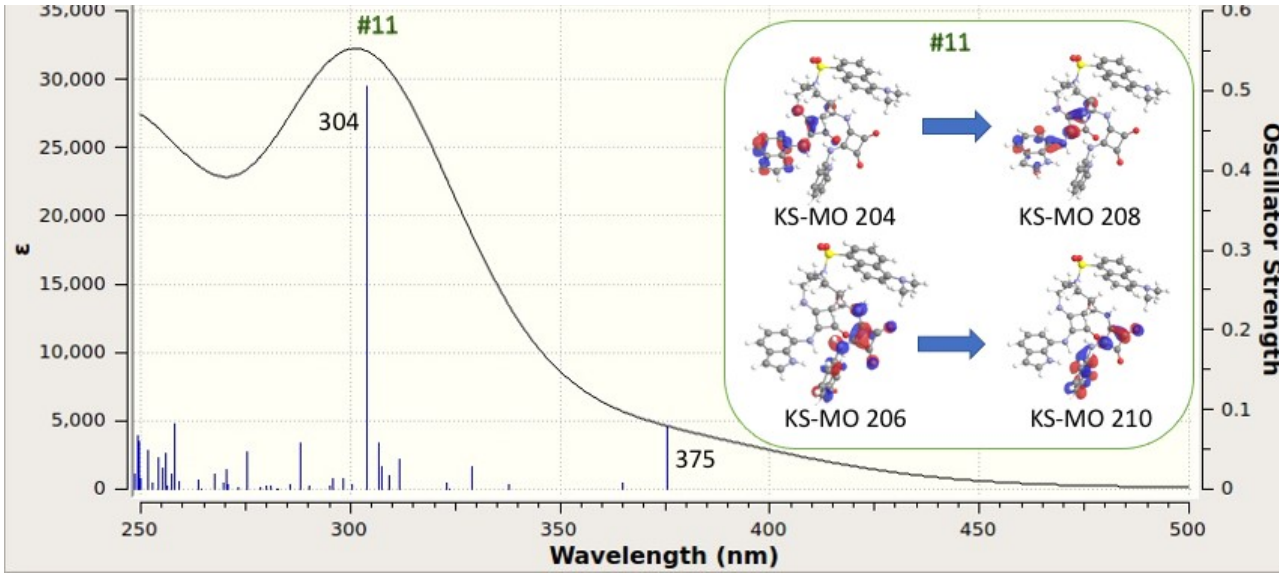

Figure S43. UV-Vis spectrum (250–500 nm) simulated for **L4** based on TD-DFT calculations. In the inset, the Kohn-Sham molecular orbitals (KS-MO) involved in the main monoelectronic transition contributing to the GS⟶ES #11 are reported.

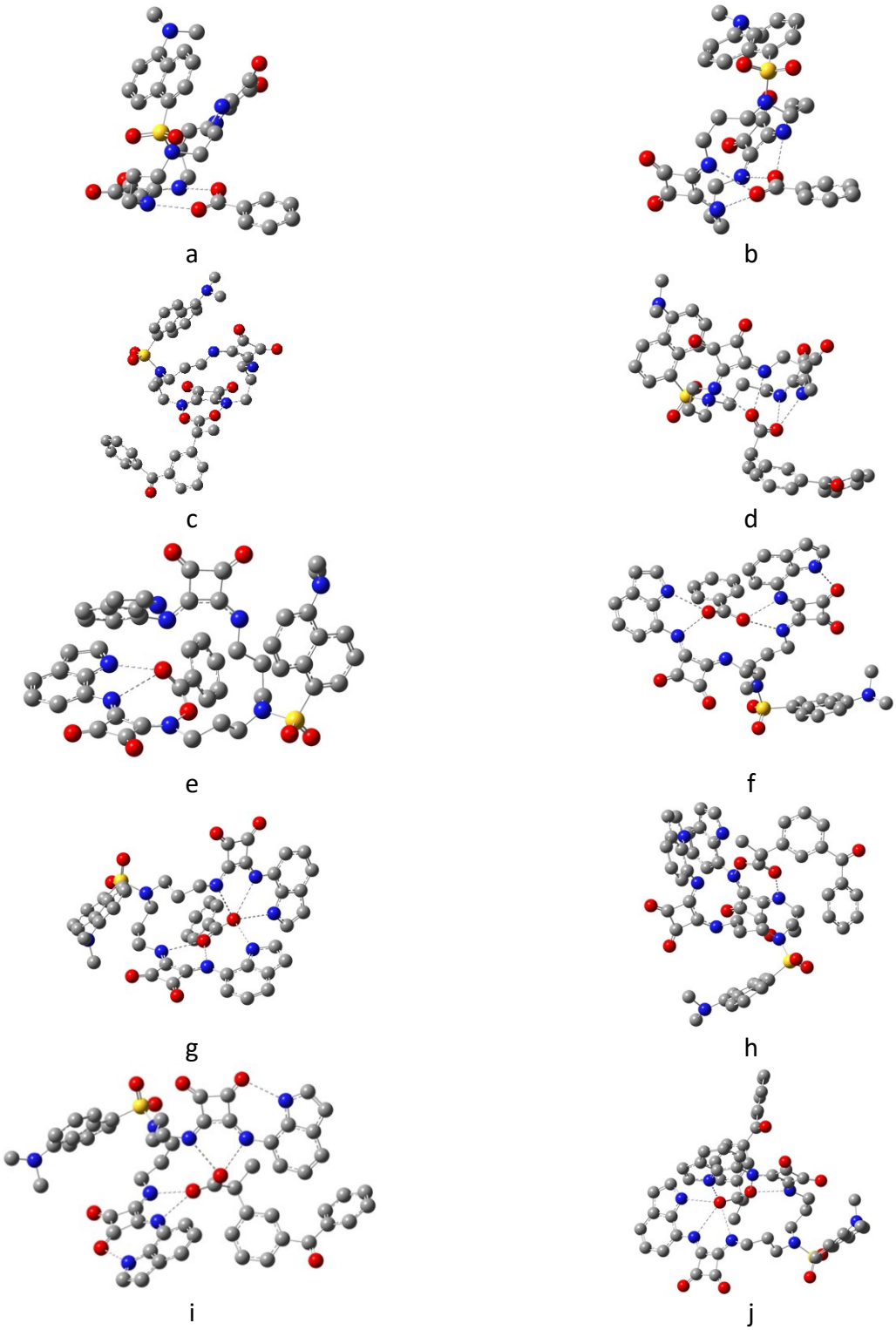

Figure S44. Optimized geometries of the 1:1 adducts formed by **L2** (entries a–d) with BzO^- (a, b) and KET^- (c, d) and by **L4** (e–j) with BzO^- (e–g) and KET^- (h–j). Hydrogen atoms were omitted for clarity. Only the HB interactions with N···O distances shorter than 3.1 Å are depicted as dashed lines. Energy data and TD-DFT results for each entry are summarized in Table 2.

In order to verify the binding ability of **L4** to form 2:1 anion:receptor adducts, four different conformations of the **L4**·2BzO$^-$ adduct (entries a-d in Table S2) were optimized, differing for the number and type of HB interactions, and involving or the squaramide N–H groups in both pendants, or all the squaramide and the indole N–H HB donors, or different combinations of the two coordination modes. As expected, the most stable conformation was achieved when all the available N–H groups interact with the carboxylate terminal group of the anion (entry c in Table S2 and Figure S45). Notably, all conformations display very similar electronic absorption features in the UV-Vis region (lmax = 327–334 nm, $\varepsilon = 45\cdot10^3 – 55\cdot10^3$ M^{-1} cm^{-1}). Based on these findings, the adduct **L4**·2KET$^-$ was also optimized by hypothesising a coordination mode analogous to the most stable identified for **L4**·2BzO$^-$, and subsequently investigated at TD-DFT level (entry e in Table S2). Summarily, **L4** was proved to be able to simultaneously interact with either two BzO$^-$ or two KET$^-$ anions, as experimentally found based on ^{1}H-NMR spectroscopy. The interaction energy per anion is in both cases of about 45 kcal mol^{-1}, *i.e.* about 30% lower than that calculated for 1:1 adducts discussed in the main manuscript (Table 2) as a consequence of the lower number of HBs established by the receptor with each anionic unit.

Table S2. Total electronic energies (*E*, Hartree), maximum absorption wavelength (λ_{max}, nm)[a] and relevant molar extinction coefficient (ε, 10^3 $M^{-1}\cdot cm^{-1}$),[a] adduct stabilization energies (ΔE, kcal·mol^{-1}) per anion unit in the adducts *a*–*e* between the receptor **L2** and the anions BzO$^-$ (*a*–*d*; see Figure S45) and KET$^-$ (*e*) optimized at DFT level.

Entry	Adduct	*E*	λ_{max}[a,b]	ε	ΔE
a	**L4**·BzO$^-$	-3749.3375	334	45	34.73
b		-3749.3643	328	52	43.14
c		-3749.3699	332	47	**44.90**
d		-3749.3590	327	55	41.48
e	**L4**·KET$^-$	-4594.5972	334	44	**45.96**

[a] λ_{max} and ε value obtained from the convolution of the electronic excitations assuming a half-band width of 0.333 eV. [b] λ_{max} = 249 and 304 nm for **L2** and **L4**, respectively.

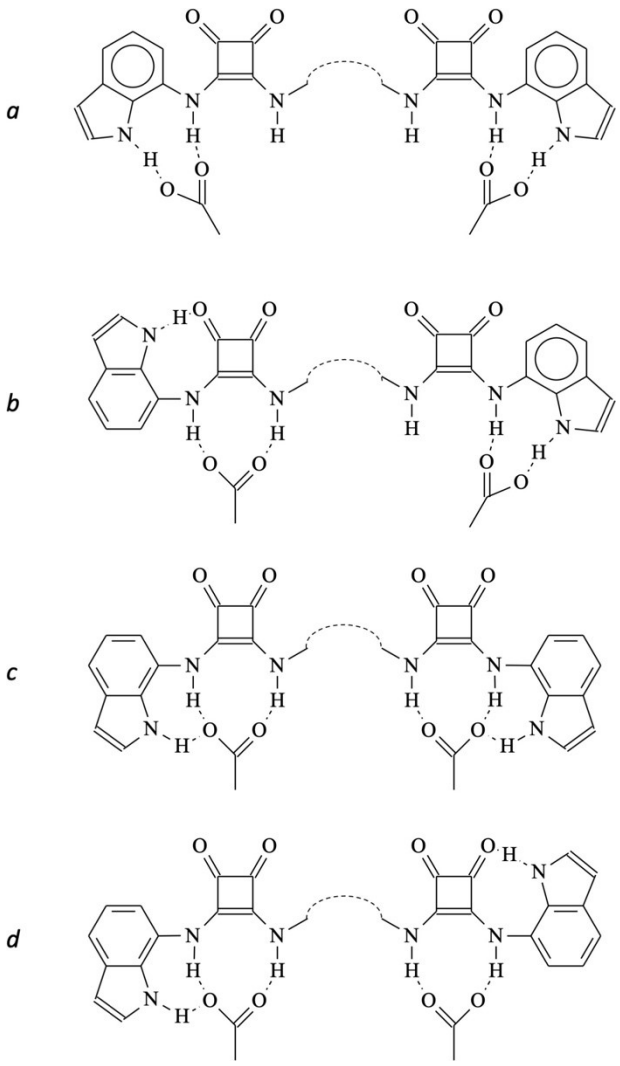

Figure S45. Schematic representation of the interaction modes of the squaramide pendants of receptor **L4** with carboxylate groups of the BzO^- anions optimized at DFT level (Table S2).

6. Note on the effect of the counter cation:

To evaluate the possible interference of the counter cation in the host-guest interaction between the receptors and the target anions tested, we performed fluorescence measurements of **L1** and **L2** by adding a competitive salt (i.e. $NaBF_4$ and NaOTf) in the presence and the absence of sodium ketoprofen. As shown in Figures S46a-d, the presence of $NaBF_4$ and NaOTf does not affect the host-guest interaction occurred between the receptor and the sodium ketoprofen. Indeed, in both cases for **L1** and **L2**, the addition of the KET^- (10 equivs) caused the partial quenching of the receptor (red line), whereas the addition of the competitive salt (green line) does not cause significant changes in the fluorescence spectrum of the free receptor (black line). Furthermore, the addition of the competitive salt to a solution of the receptor in the presence of sodium ketoprofen does not cause any significant change in the spectrum (yellow line).

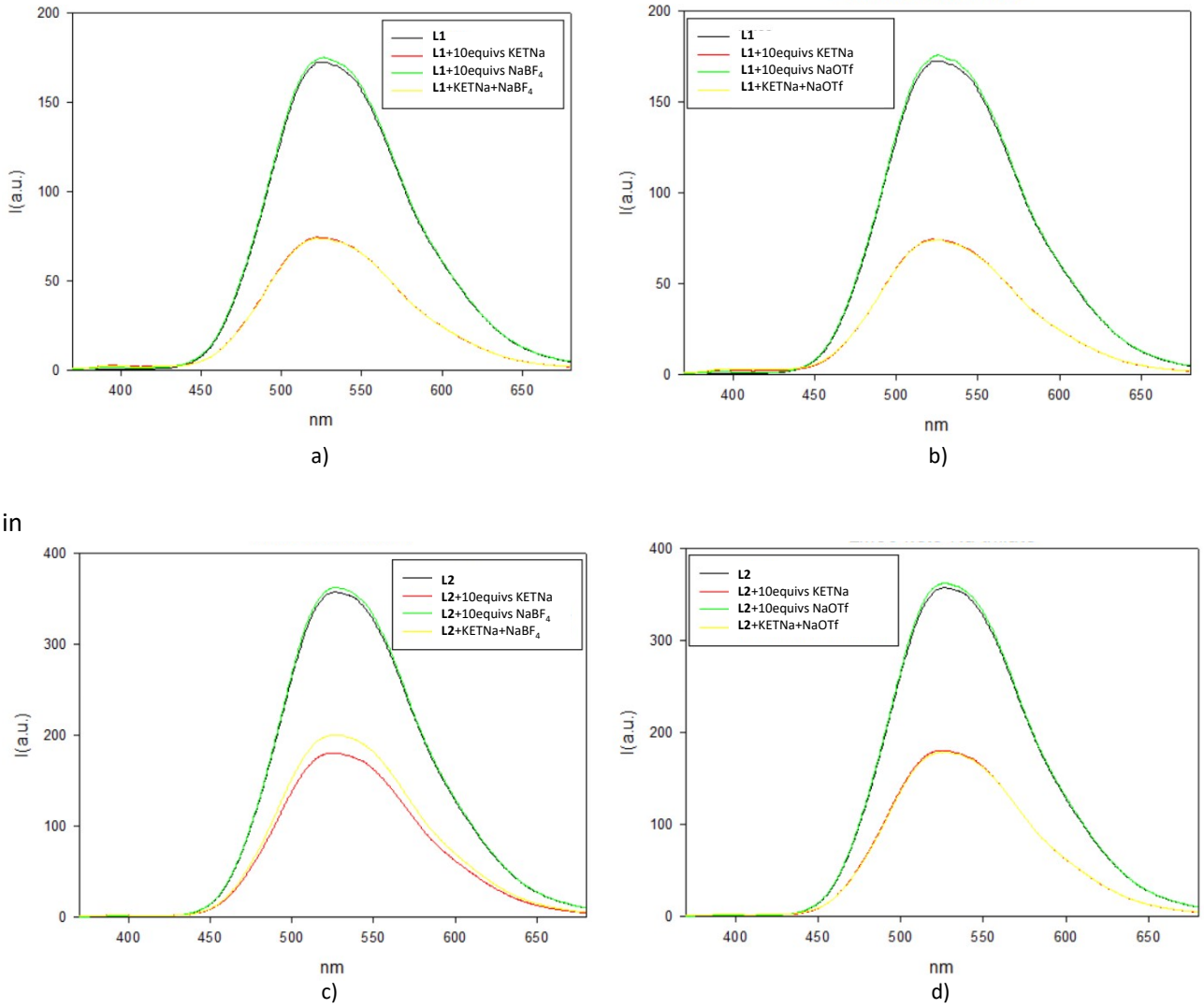

in

Figure S46. Effect of $NaBF_4$ a) and c) and NaOTf b) and d) on the fluorescence spectra of **L1** and **L2** and their adducts with KETNa in CH_3CN/DMSO (9:1 v/v).

The behaviour observed demonstrated that the sodium cation does not affect the fluorescence response of the two systems. To further support these findings, we also conducted fluorescence measurements in the presence of $TBABF_4$, and the behaviour was identical to that observed with $NaBF_4$ (Figure S47).

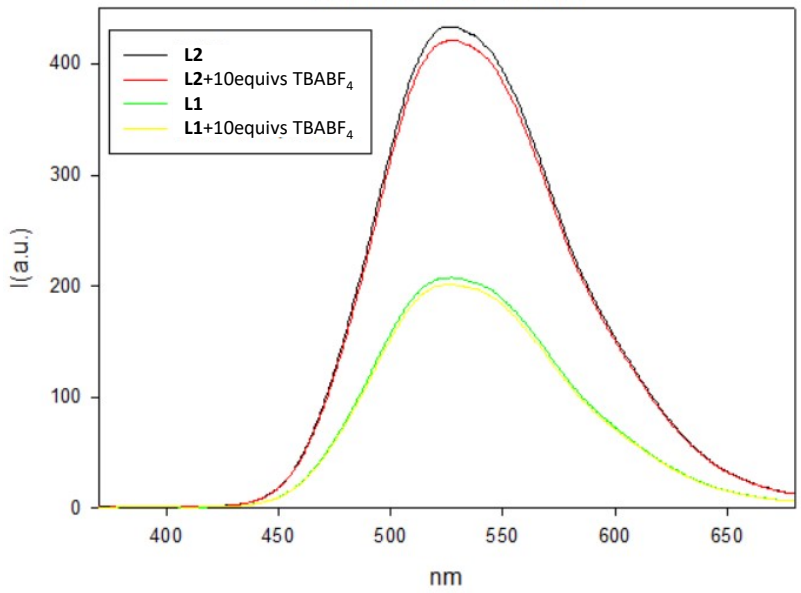

Figure S47. Fluorescence spectra of **L1** and **L2** in the presence of 10 equivs of $TBABF_4$ in CH_3CN/DMSO (9:1 v/v).

In the case of **L4**, the changes in UV-Vis and fluorescence are identical in the presence of TBABzO and NaBzO (Figure S48).

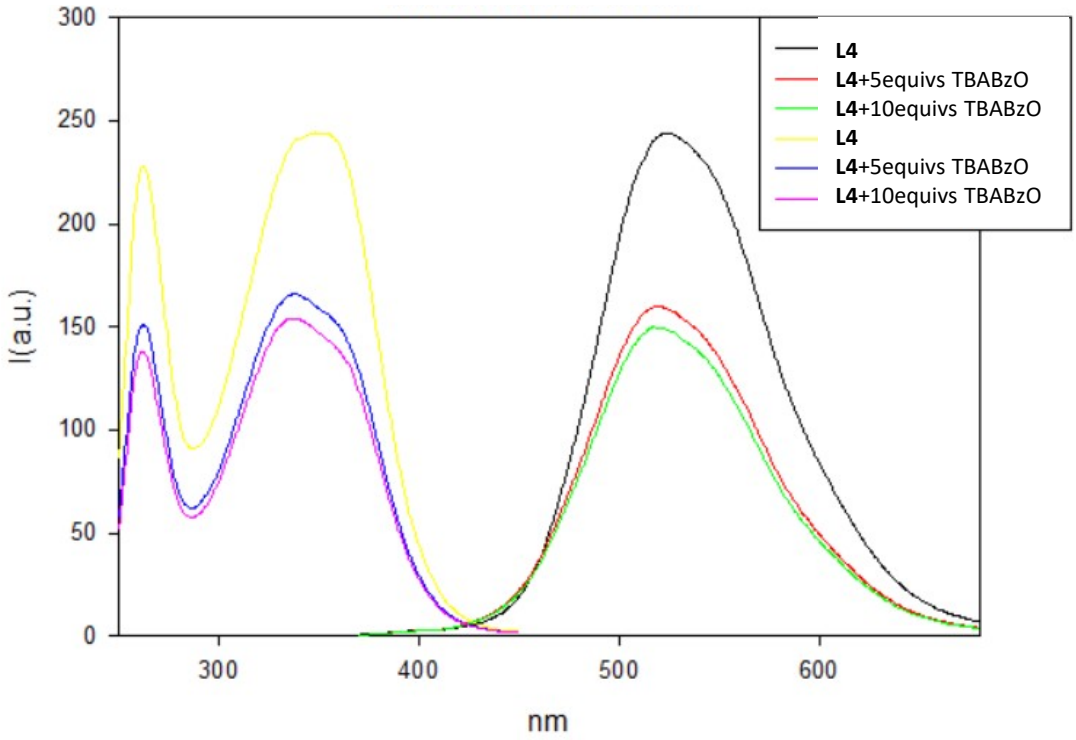

Figure S48. Excitation (yellow, blue, and pink lines), and emission (black, red, and green lines) spectra of **L4** in the presence of 5 and 10 equivs of TBABzO in CH_3CN/DMSO (9:1 v/v).

Furthermore, we conducted ^{1}H-NMR titrations in DMSO d_6/0.5% water in the presence of TBABzO (Figure S39). The calculated association constant is comparable to that calculated in the presence of BzONa (see Table S1), confirming that the influence of the counter cation is negligible.